Results in Engineering 23 (2024) 102503

Contents lists available at ScienceDirect

Results in Engineering

journal homepage: www.sciencedirect.com/journal/results-in-engineering

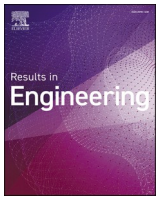

Eco-friendly mix design of slag-ash-based geopolymer concrete using explainable deep learning

R.S.S. Ranasinghe [a], W.K.V.J.B. Kulasooriya [a], Udara Sachinthana Perera [a], I.U. Ekanayake [b,c], D.P.P. Meddage [d], Damith Mohotti [d,e], Upaka Rathanayake [f,*]

[a] Department of Civil Engineering, Sri Lanka Institute of Information Technology, Malabe, Sri Lanka
[b] School of Computing Technologies, Royal Melbourne Institute of Technology, Melbourne, VIC, Australia
[c] Ceylon Institute for Artificial Intelligence Research (CIAIR), Colombo, Sri Lanka
[d] School of Engineering and Information Technology, University of New South Wales, Canberra, Australia
[e] School of Civil, Mining and Environmental Engineering, Faculty of Engineering and Information Sciences, University of Wollongong, Wollongong, NSW, 2522, Australia
[f] Department of Civil and Environmental Engineering, Atlantic Technological University, Ireland

ARTICLE INFO

Keywords:
Geopolymer concrete
Compressive strength
Artificial intelligence
Deep learning
Explainability

ABSTRACT

Geopolymer concrete is a sustainable and eco-friendly substitute for traditional OPC (Ordinary Portland Cement) based concrete, as it reduces greenhouse gas emissions. With various supplementary cementitious materials, the compressive strength of geopolymer concrete should be accurately predicted. Recent studies have applied deep learning techniques to predict the compressive strength of geopolymer concrete yet its hidden decision-making criteria diminish the end-users' trust in predictions. To bridge this gap, the authors first developed three deep learning models: an artificial neural network (ANN), a deep neural network (DNN), and a 1D convolution neural network (CNN) to predict the compressive strength of slag ash-based geopolymer concrete. The performance indices for accuracy revealed that the DNN model outperforms the other two models. Subsequently, Shapley additive explanations (SHAP) were used to explain the best-performed deep learning model, DNN, and its compressive strength predictions. SHAP exhibited how the importance of each feature and its relationship contributes to the compressive strength prediction of the DNN model. Finally, the authors developed a novel DNN-based open-source software interface to predict the mix design proportions for a given target compressive strength (using *inverse modeling* technique) for slag ash-based geopolymer concrete. Additionally, the software calculates the Global Warming Potential (kg CO_2 equivalent) for each mix design to select the mix designs with low greenhouse emissions.

1. Introduction

Concrete is widely used in construction because of its durability, strength, and low cost. However, Ordinary Portland Cement (OPC), the main ingredient in concrete, emits about 2.4 billion tons of CO_2 each year, contributing significantly to global warming [1]. To reduce these emissions, the construction industry is looking at alternative materials to replace or enhance traditional Portland cement [2]. One such alternative is geopolymer concrete, which has a lower carbon footprint because it replaces OPC [3]. Geopolymers are inorganic materials made from alkali aluminosilicate and have a different composition from traditional concrete [4] but can still match or even exceed the durability of OPC, particularly in acidic, sulphate, and chloride environments. It has demonstrated the ability to match conventional Ordinary Portland Cement (OPC) in terms of resilience in acidic, sulphate, and chloride environments and the ability to survive thermal exposure conditions under aggressive environmental conditions [5]. Diaz-Loya et al. [6] reported that mechanical properties such as compressive strength, poisons' ratio, and flexural strength of fly ash-based geopolymer concrete were comparable with ordinary Portland cement concrete. Geopolymer concrete is also more durable, especially in coastal environments, making it a strong and sustainable alternative to traditional concrete [7].

Generally, repetitive laboratory experiments are required to obtain the desired strength characteristics of any given concrete mix. As geopolymer concrete has many constituents, a rigorous experimental program is required to observe their impact on mechanical strength

* Corresponding author.
E-mail address: Upaka.Rathnayake@atu.ie (U. Rathanayake).

https://doi.org/10.1016/j.rineng.2024.102503
Received 22 February 2024; Received in revised form 27 May 2024; Accepted 1 July 2024
Available online 2 July 2024

Abbreviations

AG	Aggregates
GGBFS	Ground Granulated Blast Furnace Slag
AD	Admixture
HD	Heating Degree
AL	Alkali Liquid
LP	Limestone Powder
ANN	Artificial Neural Network
M	Molarity
AS	Alkaline Solution
MAE	Mean Absolute Error
AV	Admixture of modified Viscosity
MC	Molarity Concentrations
B	Binder
MFNN	Multi-layer Feedforward Neural Networks
BP	Back Propagation
MP	Marble Powder
BS	Basaltic
MSE	Mean Squared Error
C	Cement
n	Porosity
CA	Coarse Aggregates
NS	Nano Silica
CC	Cascade Correlation
NZ	Natural Zeolite
CCA	Corncob Ash
PF	Polypropylene Fibers
Z	Zeolite
PV	P-Wave Velocity
CD	Curing Days
R	Correlation Coefficient
CG	Concrete strength grade
R^2	Coefficient of Determination
CH	Curing Humidity
RA	Rise-husk Ash
CiR	Chipped Rubber
RCA	Recycled Coarse Aggregates
CNN	Convolution Neural Network
ResNet	Residual Networks
CoA	Concrete Age
RPA	Recycled Plastic Aggregates
CP	Calcite Powder
RPCR	Replacement Ratio
CR	Crumb Rubber
S	Superplasticizer
CS	Compressive Strength
SA	Sample Age
CSH	Concentration of Sodium Hydroxide
SD	Saturated Surface Dried Density
CT	Curing Temperature
SF	Silica Fume
DNN	Deep Neural Network
SH	Schmidt Hammer
FA	Fine Aggregates
SHP	Sodium Hydroxide Pellets
FB	Fractional Bias
SN	Sand
FAS	Fly Ash
SSG	Sodium Silicate Gel
FRPCR	Fly Ash Replacement Ratio
W	Water
FPNN	Fuzzy Polynomial Neural Networks
WA	Water Absorption
GR	Gravel

characteristics. This repetitive task requires more time and expertise to obtain reliable results. Therefore, the engineering community has used analytical methods in predicting strength characteristics at the initial stage of the mix-design trials. One such method is to use data-driven approaches such as machine learning.

Many researchers have used machine learning models to accurately predict geopolymer concrete's strength characteristics [8–10]. Despite the accurate predictions of machine learning models, its less transparency in the decision making process stands as an obstacle in practical usage [11]. For example, once the prediction was obtained, the reason how the model came up with it was partially or completely unknown. As a solution, explainable artificial intelligence (XAI) techniques were introduced to interpret the complex machine learning models and their prediction process. XAI has recently been employed in studies that developed classical machine-learning models to predict the compressive strength of concrete [12].

On the other hand, many related works that predicted the properties of geopolymer concrete have often used deep learning algorithms (a subset of machine learning) such as deep neural networks and convolutional neural networks [9,10]. Nevertheless, XAI has been very limitedly used for deep learning models in the general concrete domain. As deep learning models can learn complex patterns in the mix design data, using XAI for these models can precisely estimate how each constituent of the mix design influences the characteristics of geopolymer concrete. Because geopolymer concrete has multiple components in the mix design, XAI can help optimize the mix design, avoiding rigorous experimental work. Therefore, this study investigates the use of deep learning models with XAI to predict the compressive strength of slag ash-based geopolymer concrete.

2. Related work

Machine learning (including deep learning methods) has been frequently employed in predicting the strength characteristics of concrete, as well as geopolymer-based concrete. Pazouki [13] used a radial basis function neural network (RBFNN) with an ant colony optimization algorithm (ACO), the group method of data handling (GMDH) and an artificial neural network (ANN) to predict the Characteristics Strength of fly ash based geopolymer concrete. All three models demonstrated reasonable performance in predicting the mechanical properties of fly ash-based geopolymer concrete, and RBFNN exhibited the best performance. Nguyen et al. [14] have modeled the compressive strength of fly ash-based geopolymer concrete by using deep neural networks (DNN) and Residual Networks (ResNet). Both the ResNet and DNN have exhibited high fitting accuracy of $R^2 = 0.985$ and $R^2 = 0.970$ respectively. Using three machine learning algorithms (support vector machine (SVM), backpropagation neural network (BPNN), and extreme learning machine (ELM)), Peng & Unluer [15] predicted the characteristic compressive strength of geopolymer concrete using different mix proportions with pre-curing conditions. The R^2 values for SVM, BPNN, and ELM predictions are 0.914, 0.932, and 0.914, respectively. Shahmansouri et al. [16] investigated the impact of partially replacing granulated blast-furnace slag with silica fume and natural zeolite on the compressive strength of geopolymer concrete by using an ANN approach. The ANN model accurately predicted the compressive strength with a low mean squared error (MSE) of 9.53 and a high R^2 of 0.95. Recently, a study was conducted using eight machine learning models to predict the compressive strength of calcium-based geopolymer concrete. Among those, the extreme gradient boosting (XGB)

model exhibited the highest prediction accuracy of 91 %, and the root mean square error(RMSE) was 3.85 [17]. Rahmati and Toufigh [18] used SVR and ANN to model the compressive strength of geopolymer concrete exposed to high temperatures. Ahmad et al. [19] used an Adaptive boosting (AdaBoost) regressor, decision tree (DT), and bagging regressor (BR) to predict the compressive strength of geopolymer concrete made with fly ash. In this study, BR stood out as high accurate prediction model with an R^2 value of 0.97. Huynh et al. have employed DNN, ANN, and ResNet to predict the compressive strength of fly ash-based geopolymer concrete [20]. Out of the three models, ResNet exhibited high accuracy in strength prediction with R^2 of 0.937. Cao et al. [21] modeled the compressive strength of fly-ash-based geopolymer concrete by using multilayer perceptron (MLP), SVM, and XGB models. The findings revealed that XGB outperformed the other models by achieving an R^2 value of 0.98.

The authors noted that ANN-based deep learning models had been frequently used in investigating strength characteristics modeling of concrete, including geopolymer concrete as they often yield higher predictive accuracies. Table 1 summarises the work that used deep learning methods (neural networks) for concrete-related strength predictions in reverse chronological order. However, most deep learning models are complex and less interpretable. In this occasion, XAI is critical as it provides the underlying reasoning behind predictions. The use of XAI has been popular in classical machine learning models used for concrete strength prediction (e.g., tree models, SVM) [11,21–23]. The use of explainable artificial intelligence provides confidence to its end-user by providing human comprehensible interpretations of predictions. However, the *authors noted that explainable artificial intelligence has not been adequately used in deep learning models in this context*. Recently, Choi et al. [24] used local interpretable model agnostic explanations for explaining deep neural networks. However, LIME provides local explanations (explain only a specific instance) and creates dummy instances of original instances to create the explanations. Therefore, Kulasooriya et al. [12] argued that LIME may not reveal the actual importance of the feature. Furthermore, LIME does not provide global explanations for the whole model.

To address the research gap in revealing the underlying factors of complex deep learning models, the authors utilized Shapely Additive Explanations (SHAP). Even though SHAP has been used in various deep learning applications [61,62], it has been rarely used in explaining the deep learning models and their capabilities in compressive strength predictions. It can provide a wide range of explanations of the machine learning/deep learning model. First, this study developed three deep-leaning models to predict the compressive strength of slag-ash-based geopolymer concrete. Then the features of the best-performing model were explained with the aid of SHAP. The authors utilized the best deep learning model to introduce an open-source software interface written in Python as the final output of the study. This interface takes the target compressive strength of geopolymer concrete as an input and outputs the required mix-design proportions. The underlying algorithm of the interface employs an inverse modeling technique of the trained deep learning model. Additionally, the interface indicates the global warming potential (GWP) of each concrete mix. These GWP levels guide users to select the most sustainable and eco-friendly mix design of geopolymer concrete.

3. Methods and data

3.1. Methodology of the study

The workflow of the study is presented in Fig. 1. This study used a data set of slag ash-based geopolymer concrete (260 data points) obtained from literature [63]. The dataset was divided into training (70 %), validation (10 %) and testing (20 %) to compare the performance of deep learning models. An artificial neural network (ANN), a deep neural network (DNN), and a convolutional neural network (CNN) were used as

Table 1
A collection of previous work has been done to predict concrete strength using deep learning methods.

Year	Model	Input Parameters	Dataset size	XAI used/ not	Source
2023	DNN	GGBFS (Ground Granulated Blast Furnace Slag), CCA (Corncob Ash), FA (Fine Aggregates), CA(Coarse Aggregates), W(Water), SHP (Sodium Hydroxide Pellets), SSG (Sodium Silicate Gel), CD (Curing Days), MC (Molarity Concentrations), CG(Concrete strength Grade)	260	No	[25]
2023	DNN	W, C (Cement), FAS (Fly Ash), CA (Coarse Aggregates), FA, CT (Curing Temperature), CH (curing Humidity), BFS (Blast Furnace Slag)	775	Yes - LIME	[24]
2023	ANN	AS (Alkaline Solution): B (Binder), NaOH, SiO_2: NaOH, M (Molarity), W:C, FAS: GGBFS	1030	No	[26]
2023	ANN	AS, AG (Aggregates), NaOH, FA, CT (Curing Temperature), CD, Na_2SiO_3, NaOH: Na_2SiO_3, SiO_2:Al_2O_3	510	No	[27]
2023	ANN	A, RPA (Recycled Plastic Aggregates), NS (Nano Silica), NaOH, M, CoA (Concrete Age), CD, AS	207	No	[28]
2023	ANN	AG, RPA, NC, NaOH, CoA, CD, AS	210	No	[29]
2022	ANN	AS, AG, NaOH, FAS, M, NaOH: Na_2SiO_3, SiO_2:Al_2O_3, GGBFS, SiO_2: CaO	220	No	[30]
2022	ANN	W:C, RCA, CT, CD, W, S (Superplasticizer), C	61	No	[31]
2021	ANN, DNN	Specimen Type, C, B, S, W, W:C, W: B, FA, CA, CR (Crumb Rubber), CiR (Chipped Rubber)	233	No	[32]
2021	ANN	SF (Silica Fume), NaOH, GGBFS, SA (Sample Age), NZ (Natural Zeolite)	117	No	[16]
2021	ANN	C, S, AG, W, SA, GGBFS, FAS	1030	No	[33]
2021	LSTM, DNN	SH (Schmidt Hammer), n (Porosity), PV (P-wave Velocity), Point Load index	170	No	[34]
2020	DNN, ResNet	FA, W glass solution, NaOH, CA, Concentration of NaOH, CD, CT	335	No	[9]
2020	ANN	SA, GGBFS, A, S, W, FAS, C	2817	No	[35]
2020	DNN, ANN, ResNet	FAS: AG, CT, CD, NaOH: Na_2SiO_3, AL (Alkali Liquid): FA, CSH (Concentration of Sodium Hydroxide),	263	No	[36]
2019	ANN	W, NaOH, FAS, Gel base Na_2SiO_3	210	No	[37]
2019	ANN	C, FA, W, RA (Rise-husk Ash), AV (Admixture of modified Viscosity), AG, GGBFS, CP (Calcite Powder), SF	205	No	[38]
2018	ANN	Weight of W, C, W:C, AG nominal maximum size, CT, CA and FA composite specific gravity, WA (Water Absorption) of FA and CA, Fine Virgin aggregates, Fine Reclaimed Asphalt Pavement, Coarse Virgin Aggregates, RA	66	No	[39]

(*continued on next page*)

Table 1 (*continued*)

Year	Model	Input Parameters	Dataset size	XAI used/ not	Source
2018	ANN	WA, W:C, FA, Natural CA, RCA (Recycled Coarse Aggregates) AG, W: Total Materials	139	No	[40]
2018	ANN	SA, GGBFS, AG, S, W, FA	1133	No	[41]
2016	ANN	C, FA, NS, Cu Slag, CoA, S, CA, W:C	264	No	[42]
2016	ANN	C, W, AG, CD, Micro Air	144	No	[43]
2016	ANN	W:C, FA:C, CA:C	76	No	[44]
2014	ANN	AG, Natural and Recycled FA, C, Natural CA-10, 20 mm, Recycled CA-10, 20 mm, W, W:C, AD (Admixture), AG:C, S: A, RPCR (Replacement Ratio), W: Total Materials	257	No	[45]
2013	ANN	W, SN (Sand), Fitness Modulus of SN, Natural and Recycled CA, C, W:C, WA, SD (Saturated Surface Dried Density), RPCR, Maximum Size, Impurity of RCA, Coefficient of Specimen	146	No	[46]
2013	ANN	–	1178	No	[47]
2012	ANN	C, FAS, HD (Heating Degree), PF (Polypropylene Fiber), A, MP (Marble Powder), Natural AG, BS (Basaltic), LP (Limestone Powder), Z (Zeolite)	85	No	[48]
2011	ANN	FA, C, CA, W, W: Powder, S, FAS, Bottom Ash	80	No	[49]
2010	ANN	S, SA, GGBFS, AG, W, FAS	300	No	[50]
2009	ANN	C, W, AG, SA, GGBFS, S	225	No	[51]
2009	ANN, BP	SN, W:C, FA, CA, SF, S, CD	–	No	[52]
2009	ANN	Aggregate Age, C, GGBFS	284	No	[53]
2008	ANN	C, W, S, Crushed Stone, high range W reducing agent, CaO, FAS	180	No	[54]
2008	FPNN	C, W, FA, CA, S, SF,	458	No	[55]
2008	ANN	W, C, Steel Fiber, W:C, Pumice S & GR (Gravel), S	126	No	[56]
2007	ANN	FAS, SF, C, FA, CA, W, SA, High-Rate Water Reducing Agent	144	No	[57]
2006	ANN	S, SF, AE (Air-entraining Agent Ratio), FA, W:C, FAS	187	No	[58]
2001	ANN	C, W, FA, CA, SF	93	No	[59]
2000	MFNN	C Grade, W:C, W, C, CA size, S fine modulus, S: A, A:C, AD	65	No	[60]

deep learning models in this study as these models have been commonly used in the state-of-the-art.

Conducting a thorough evaluation of their performances is critical to identify the best-performed model. In order to evaluate the predictive performance, generally used error indices and statistical methods were employed. These methods ensure the reliability and consistency of the predictions compared to the experimental data. Once the best model is obtained, SHAP (Shapley Additive exPlanations) was applied to generate model explanations: global (model in whole), local (specific instance), and feature dependency (impact of individual input parameters) for the best-performed deep learning model. These explanations were methodically examined to determine how the deep learning model makes the decision, revealing its underlying reasoning behind predictions. Additionally, a novel software interface was developed using inverse modeling techniques by using the best-performing deep learning model. This tool was designed to predict the mix designs of geopolymer concrete that result in the lowest carbon emissions. For example, once the target strength is provided, the tool itself provides possible combinations of inputs that can achieve the target strength (considering a threshold value). Subsequently, the tool ranks the mix designs based on Global Warming Potential (GWP) in terms of $kgCO_2$ equivalent. Therefore, unlike a typical prediction tool, the novel tool provides all possible combinations that can lower the adverse impact on the environment.

3.2. Deep learning models

In this study, the authors used three different deep learning models, an Artificial Neural Network (ANN), a Deep Neural Network (DNN), and a 1D Convolutional Neural Network (CNN). All the models were compiled using Python programming with Tensorflow and Keras [64]. Table 2 presents the summary of the model architecture of three deep learning models. Moreover, their proposed model architecture is shown in Fig. 2.

3.3. Explainable artificial intelligence (XAI)

Explainable Artificial Intelligence (XAI) focuses on making the decision-making processes of complex machine learning models more understandable to humans [65–70]. XAI can be viewed in two major groups based on the model's complexity. First group: Intrinsic model explanations which are suitable for simpler models like linear regression and decision trees [71–73]. These models can directly show how input features affect their output (the model itself is explainable), making it easy to understand their decision logic. However, explaining how these models arrive at their predictions becomes challenging in the second category, which involves complex model structures such as neural networks or ensemble methods. Complex models are often more accurate than simpler ones but those models lack the transparency in explaining their reasoning. In such cases, post-hoc explanation methods are essential to provide human-understandable explanations for the predictions made by these complex machine learning models. For our specific study, we employed Shapley Additive Explanations (SHAP).

3.3.1. Shapley additive explanations (SHAP)

SHAP was introduced by Lundberg & Lee [73] as a solution to the lack of interpretability associated with complex models. SHAP is mainly based on the game theory concept, which addresses how individual members of a group (players) contribute to certain tasks (game). SHAP extends this idea by considering the contribution of each feature that influences the model's target output. This approach helps in understanding the relative importance of different input features in making predictions. By using SHAP, the importance and impact of the mix design parameters on the compressive strength of slag ash-based geopolymer concrete can be explained.

3.4. Data description

The accuracy of a machine learning approach relies on the quality and reliability of data. The authors employed a dataset of slag ash-based geopolymer concrete (260 data points) reported by Oyebisi and Alomayri [63]. Altogether there were 11 parameters in the dataset (Ground Granulated Blast Furnace Slag, GGBFS; Corncob Ash, CCA; Fine Aggregates, FA; Coarse Aggregates, CA; Water, W; Sodium Hydroxide Pellets, SHP; Sodium Silicate Gel, SSG; Curing Days, CD; Molarity Concentrations, MC; Concrete Strength Grade, CG; Compressive strength, CS). The descriptive statistics of the dataset are shown in Table 3. Notably a zero variance was observed in SSG and CA, implying a constant value throughout the dataset. The ground granulated blast furnace slag and corncob ash have the highest sample variance. Their mean values, standard deviations, and minimum and maximum values are comparable. Fine aggregate content had a mean of 818 kg/m^3, standard deviation of 56.9 kg/m^3 ranging from 728 kg/m^3 to 899 kg/m^3. The predictive variable compressive strength (CS) has a mean value of 35.9 MPa with a standard deviation of 12.2 MPa. It ranges from 11 MPa (minimum) to 64 MPa (maximum).

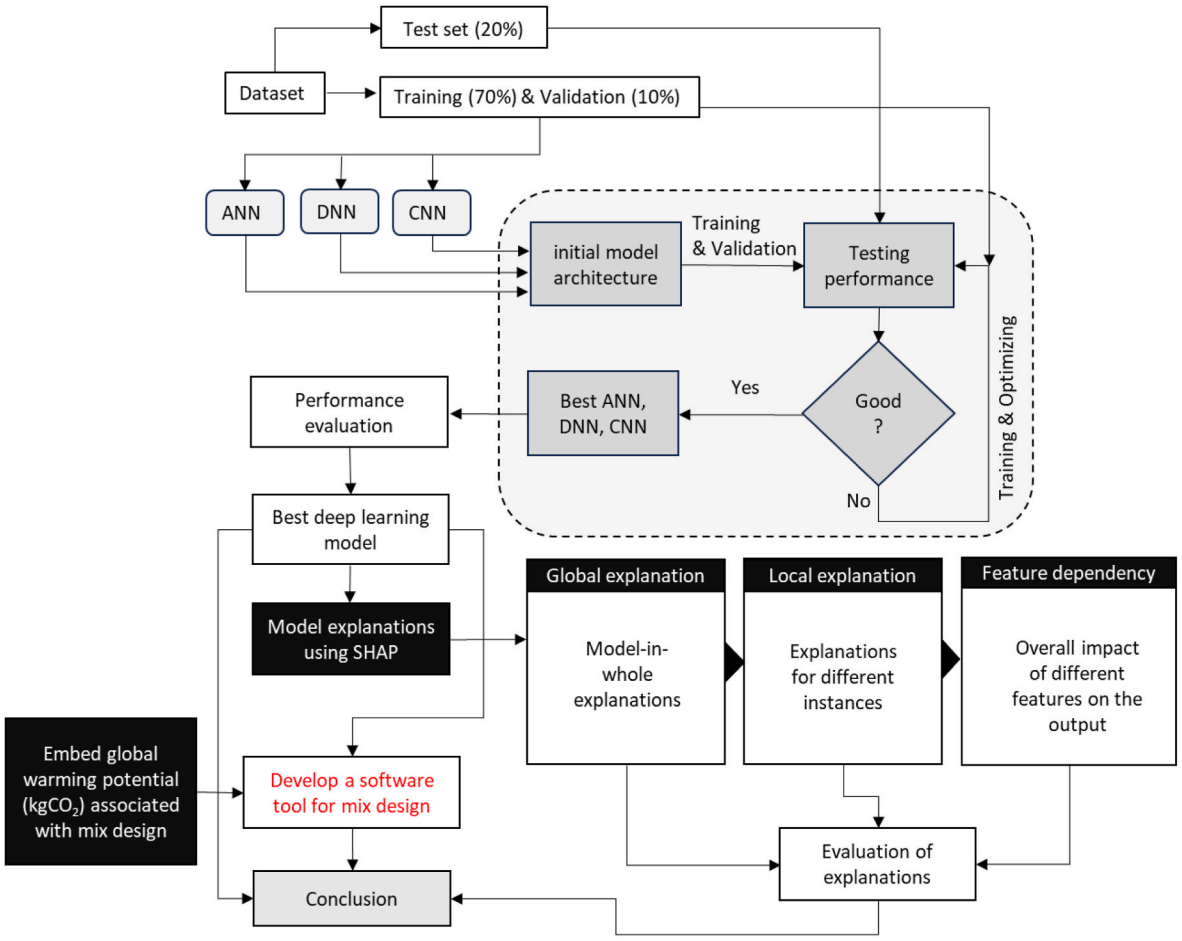

Fig. 1. Methodology of the study.

Table 2
Configuration of the deep learning algorithms.

Model	Architecture	Activation	Slope coefficient for activation	Dropout rate	Optimizer	Batch Size	Epochs
ANN	Input Layer: 8 nodes, Two Hidden Layers, 300 neurons each. Output Layer: 1 node	Leaky ReLU	0.2	0.1	Adam	500	50
DNN	Input Layer: 8 nodes, Four hidden Layers, 100 neurons each. Output Layer: 1 node	Leaky ReLU	0.2	0.1	Adam	1000	50
CNN	Input Layer: 8x1-dimensional array. Convolutional Layer: 32 filters, kernel size 3, Flattening Layer 1×192 Dense Layer: 100 Dropout Layer: 100 Output Layer: 1 node	Leaky ReLU (ReLU for 1D convolution layer)	0.23	0.2	Adam	1000	50

The pairwise plot of the correlation coefficient, R among compressive strength and other parameters are shown in Fig. 3. The R stands for the strength and direction of the linearity between each pair of variables. It ranges from −1 to 1, with −1 indicating a perfect negative correlation, 1 indicating a perfect positive correlation, and 0 indicating no correlation. According to the accepted guideline of ranges for R, |1–0.8|, |0.8–0.6|, |0.6–0.4|, |0.4–0.2| and |0.2–0| indicate strong, good, moderate, weak, and poor R between two variables under consideration respectively [74].

Ground granulated blast furnace slag displays a positive R of 0.77 with compressive strength, indicating that compressive strength tends to increase when ground granulated blast furnace slag amount is increased. This behavior has been observed by Oyebisi & T. Alomayri in their experiments [63]. Conversely, a negative correlation of −0.63 between compressive strength and corncob ash indicates that higher corncob ash values result in lower compressive strength. The poor R values of −0.10 with fine aggregates, 0.13 with coarse aggregates, and 0.09 with sodium silicate gel exhibit a weak impact of these constituents for the compressive strength of geopolymer concrete. Although the water content has a strong impact on the compressive strength of concrete, the dataset has low variance (in other words a limited range) in the water content parameter. Hence, the impact of the water content may not be accurately demonstrated in the prediction models. A moderate positive R-value of 0.42 is displayed between compressive strength and concrete strength grade. The data set only had two concrete strength grades, which may result in lower variation in that feature.

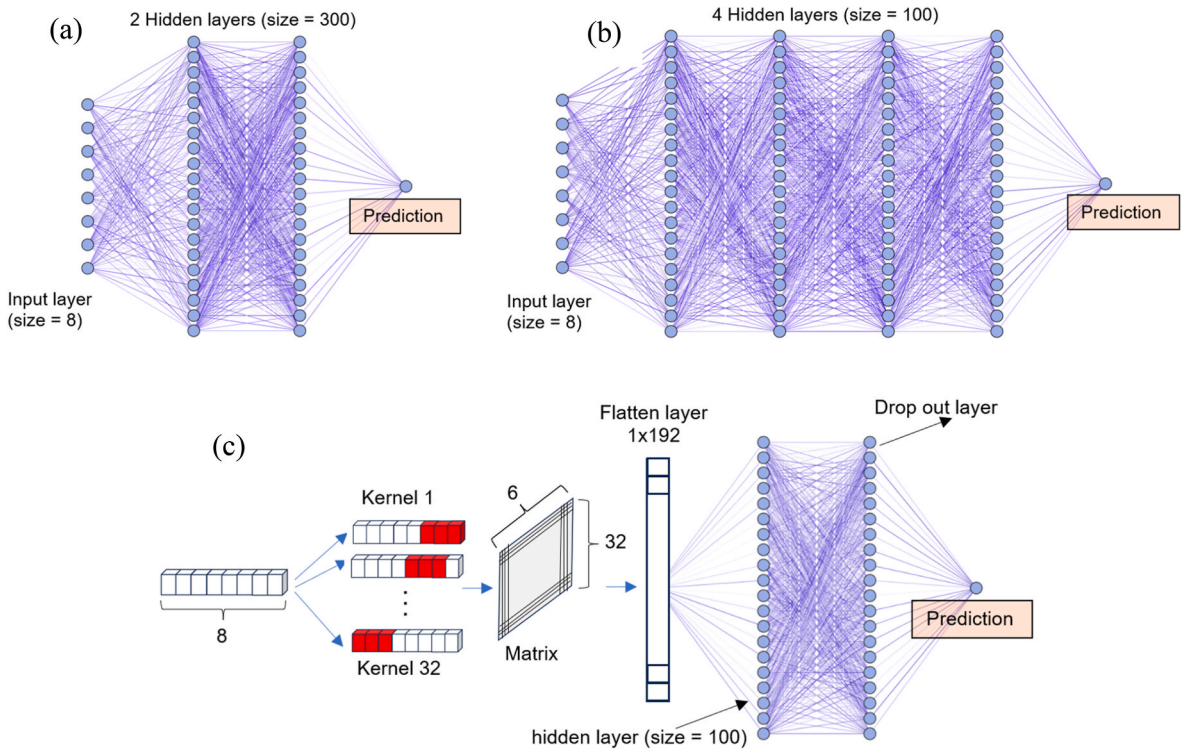

Fig. 2. The deep learning model architecture used in the study; (a) ANN (b) DNN (c) CNN.

Table 3
Descriptive statistics of the dataset.

Unit	Feature	Mean	Standard Deviation	Sample Variance	Min	Max
kg/m^3	GGBFS	218.7	153.9	23685.7	0	488
kg/m^3	CCA	215.2	152.8	23341.7	0	488
kg/m^3	FA	818.1	56.9	3237.3	728	899
kg/m^3	CA	1045.0	0.1	0.0	1044	1045
kg/m^3	W	35.2	2.2	4.6	33	38
kg/m^3	SHP	23.4	2.2	4.6	21	26
kg/m^3	SSG	146.4	0.0	0.0	146	146
days	CD	45.3	31.2	973.4	7	90
M	MC	14.0	1.6	2.7	12	16
MPa	CG	35.0	5.0	25.1	30	40
MPa	CS	35.9	12.2	148.6	11	64

Other than compressive strength, the R-value provides connections between different input variables. A high negative R-value (−0.91) between concrete grade and fine aggregates indicates that the two constitutes are negatively correlated. Similarly, the negative R-value of corncob ash and ground-granulated blast furnace slag implies that a higher amount of corncob ash is generally used with a lower amount of ground-granulated blast furnace slag. Fine aggregates and ground-granulated blast furnace slag have a weak positive R-value of 0.23, while fine aggregates and corncob ash have a moderate negative R-value of −0.55. An excellent linear relation is displayed between molarity concentrations and water, molarity concentrations and sodium hydroxide pellets, and sodium hydroxide pellets and water. Therefore, interdependencies exist in the input set. However, the exact dependency cannot be pointed out. Instead, the authors used all dependencies in the modeling as the SHAP can identify the actual dependency.

Moreover, the correlation values adhere to the findings in related work. Chi et al. [75] suggested that ground-granulated blast furnace slag can improve compressive strength and durability by reducing permeability and voids in concrete. They also highlight that adding ground granulated blast furnace slag may contribute to good workability in concrete. Ground-granulated blast furnace slag and curing days exhibit positive impacts on compressive strength, while fine aggregates demonstrate a considerable negative impact on compressive strength. Higher fine aggregate content in a concrete mix increases the water demand due to its higher surface area, resulting in a higher water-to-cement ratio which weakens the cement paste. Moreover, this high content of fine aggregates hinders proper particle packing, reducing the density of the concrete matrix and potentially increasing the porosity of a concrete mixture. This can ultimately reduce the compressive strength of concrete. In this dataset, water content has not been significantly changed (low sample variance). Therefore, it shows only a specific localized impact on the concrete.

Siddique et al. [49] mentioned that ground-granulated blast furnace slag may not improve compressive strength immediately. However, according to Nath & Sarker [76], with a curing period of 28 days, ground granulated blast furnace slag improves compressive strength. These related works also suggested that increasing ground-granulated blast furnace slag from 10 % to 30 % can significantly increase compressive strength up to 33 %, 74 %, and 110 % more than regular concrete compressive strength without ground-granulated blast furnace slag. Adesanya & Raheem, and Assefa [68,69] concluded that an increase in corncob ash would decrease the compressive strength of concrete, which agrees with pairwise correlation. Furthermore, corncob ash has low binding ability, causing it to obtain only 65 % compressive strength in 7 days compared to normal concrete [77]. These studies collectively highlight the non-linear behavior of eleven parameters with the compressive strength of geopolymer concrete, posing a challenge in predicting strength from traditional statistical approaches.

The pair-wise correlation analysis guided authors to filter unimportant parameters to develop deep learning models. Out of the ten input

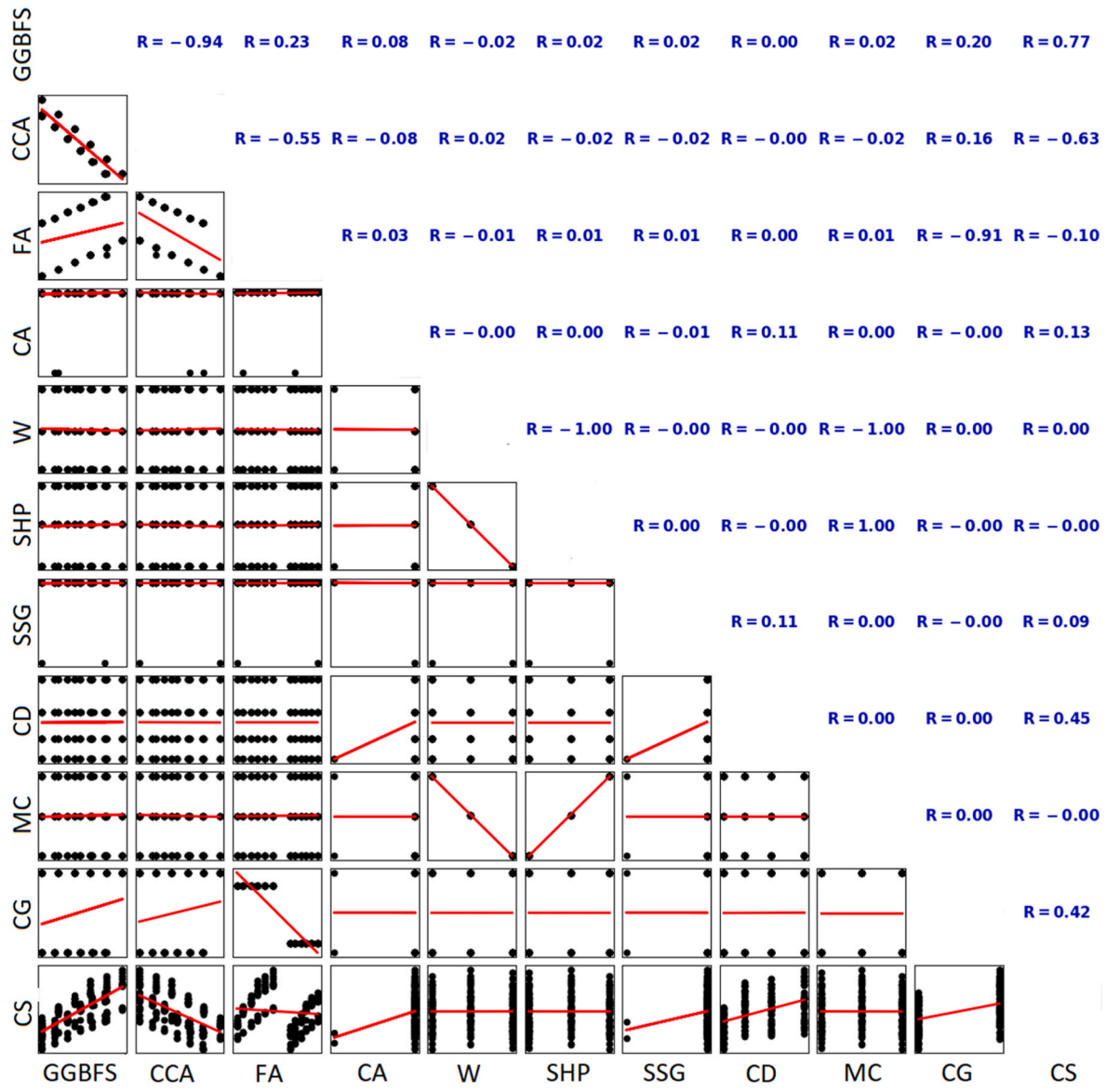

Fig. 3. Pairwise plot of R for compressive strength and mix design parameters.

parameters, coarse aggregates, and sodium silicate gel indicated a low sample variance, thus those two parameters were removed from the training dataset, to enhance model prediction efficiency.

3.5. Model optimization and performance evaluation

ANN, DNN, and CNN models were employed by splitting the data set into 70 % for training, 10 % for validation, and 20 % for testing data. All the data were normalized (*feature scaling*) and fed into the models. Feature scaling ensures better performance in neural network-based models. The model architecture of the three models was optimized using a grid search algorithm. For the grid search, the parameters such as dropout rate, learning rate, slope coefficient for activation, optimizer, and batch size were considered for all models as they govern the model performance and generalization. In addition, two parameters; kernel size and filters were considered for the 1D CNN model. Mean Absolute Error (MAE) (Equation 01), Mean Squared Error (MSE) (Equation 02), Coefficient of Determination (R^2) (Equation 03), Fractional Bias (FB) (Equation 04), and Mean Absolute Percentage Error (MAPE) (Equation 05) were used as the evaluation indices of neural network models. Each metric provides a different perspective on the accuracy and reliability of the predictions. MAE and MSE represent the magnitude of errors, with MSE being sensitive to outliers because of squaring the errors before averaging compared to MAE. Physically, MAE represents the magnitude of the errors without considering their directions. R^2 focuses on how well predictions fit the original data. FB provides a measure of proportional bias between actual and predicted values. It represents the tendency of a prediction to be systematically higher or lower than the actual values. MAPE presents a normalized measure of prediction error. In the following equations, P_i refers to the prediction obtained through each deep learning model and O_i refers to the observed value.

$$R^2 = \frac{\sum_{i=1}^{N}(P_i - O_i)^2}{\sum_{i=1}^{N}(P_i - \overline{O_i})^2} \quad (1)$$

$$MAE = \frac{\sum_{i=1}^{N}|O_i - P_i|}{N} \quad (2)$$

$$MSE = \frac{\sum_{i=1}^{N}(O_i - P_i)^2}{N} \quad (3)$$

$$FB = \frac{2(\overline{P_i} - \overline{O_i})}{(\overline{P_i} + \overline{O_i})} \quad (4)$$

$$MAPE = \frac{1}{N}\sum_{i=1}^{N}\left|\frac{O_i - P_i}{O_i}\right| \times 100\% \quad (5)$$

Following the model predictions evaluation using the error indices, a statistical evaluation was performed using a paired *t*-test. It evaluates the statistical significance of the predictions compared to the original data.

4. Results and discussion

In order to showcase how efficiently the deep learning models learn the patterns, the authors presented the training and validation loss variation considering mean squared error as the loss. Fig. 4 shows the training and validation loss curves obtained for each deep-learning model. Across all models, authors observed a rapid decrease in loss within the initial epochs, indicating a rapid learning rate during the early stages of training. Notably, the DNN model exhibits the steepest decline in validation loss, showing that its depth is beneficial for quickly capturing the underlying patterns in the dataset. By the 50th epoch, all models demonstrate a plateau in loss reduction, with the training and validation curves converging. The proximity of the training and validation curves indicates a balanced fit to the data without significant overfitting or underfitting. The loss in each model rapidly converges to a stalled value, implying an efficient learning process.

Fig. 5 illustrates the training and testing predictions obtained from each model. When considering the DNN model, most predictions fall within a 10 % error margin, with minor deviations in training and testing. Interestingly, DNN predicts extreme values (minimum and maximum) more accurately compared to the other two models. The deep layers of DNN have been useful in identifying the complex pattern in the data compared to ANN. Overall, the CNN model demonstrates reasonable predictions of compressive strength. However, a slightly more scattered nature in predictions is observed compared to the DNN. Like the DNN, CNN excels in predicting higher compressive strength values and maintains a 10 % error margin at these higher values. The ANN model shows certain deviations in the predictions, resulting in a lower accuracy than the remaining models.

Besides, the evaluations of overall predictions including training, validation, and testing are presented in Table 4. When comparing the performance of the models, the Deep Neural Network (DNN) exhibited the highest prediction accuracy, achieving a coefficient of determination (R^2) of 0.977, 0.92, and 0.972 in training validation and testing, respectively. While the DNN demonstrated the best approximation to the actual data, the other two models also displayed accurate predictive capabilities. The Convolution Neural Network (CNN) showed R^2 values of 0.939, 0.928, and 0.940, while the Artificial Neural Network (ANN) yielded R^2 values of 0.864, 0.864 and 0.854 in training, validation and testing, respectively.

The consistency of the error indices of training, validation, and testing showcases that the models have been well generalized. Moreover, the DNN achieved an MAE value of 1.93 for both training and testing. In comparison, CNN exhibited an MAE value of 2.51 for both training and testing, while the ANN had MAE values of 3.8 and 3.92. In terms of MSE, the DNN's superiority is highlighted by its values of 6.0 and 5.93 for training and testing, showcasing a 35 % improvement for both over the CNN model. However, the results do not rule out the performance of ANN and CNN models as their accuracies are acceptable. Inferior negative FB values indicate that the predictions can have minor underestimations compared to the actual compressive strength. Moreover, the Mean Absolute Percentage Error (MAPE) suggests that the DNN was the best model which obtained 3.4, 4.0, and 3.7 for training, validation, and testing. MAPE is a nondimensional error index that demonstrates the quality of the predictions. The literature suggests that MAPE <10 represents highly accurate forecasting and between 10 and 20 represents good forecasting [78]. Correspondingly, the models DNN and CNN belong to the group of highly accurate forecasting models based on MAPE. Nevertheless, all models exhibit good estimation capabilities without significant deviations. The difference between training and testing accuracies suggests that no overfits or underfits exist. For instance, a model with overfit would showcase a significantly lower testing accuracy compared to its training accuracy.

For the mean value of the predictions, a paired *t*-test was performed to evaluate whether there was a statistically significant difference. For the training set (n = 182), the paired t-tests provided the results as −0.023, 0.232, and 0.148 for the DNN, CNN, and ANN models, respectively. At a 5 % significance level, the critical t-value is ±1.96. All t-scores were well within this margin, emphasizing that there was no significant difference between the mean of predictions and the mean value of original data. The DNN model again demonstrates the closest mean to the original dataset, followed by the ANN model and the CNN model, respectively.

Similar observations were made for the paired t-tests conducted on the test sample (n = 26). It obtained t-values for the DNN model as −0.0070, for the CNN model as −0.2749, and for the ANN model as −0.3915. For a significance level of 5 %, the critical t-value is approximately ±1.708. Overall, the *t*-test confirms that the mean predictions are comparable to the mean of the original data.

In addition, Fig. 6 indicates the box plots drawn for the predictions in training and testing compared to the original (observed) data. Box plot provides a simplified representation of the data distribution. Accordingly, DNN models' distributions closely follow the distribution of observations (including mean, median, quartiles, minimum, and maximum). Minor deviations in minimum, maximum, and quartiles are observed for ANN and CNN predictions concerning the original data. Considering the performance evaluation and statistical analysis, the

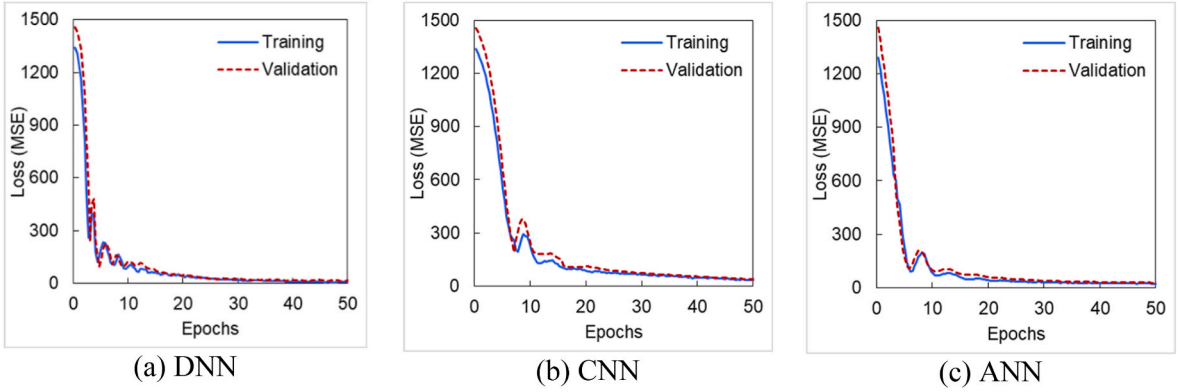

Fig. 4. Loss curves obtained for each deep learning model.

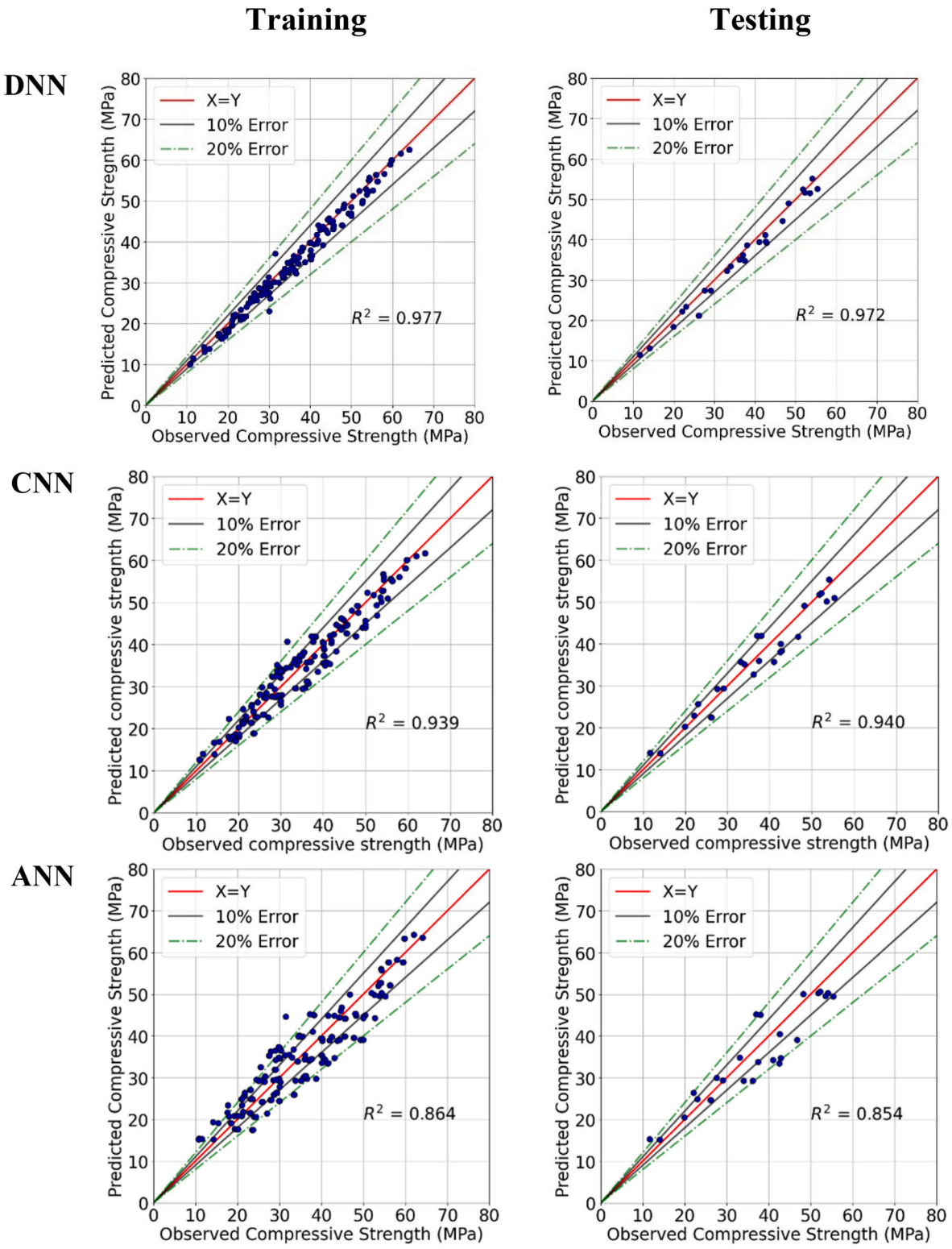

Fig. 5. Comparison of training and testing predictions.

DNN model was selected as the best-performing model for the compressive strength predictions of slag ash-based geopolymer concrete. Therefore, SHAP was used on the model DNN to explain the impact of features on the compressive strength of slag ash-based geopolymer concrete.

5. Explanations for deep learning model predictions

The authors employed Shapley additive values (SHAP) to explain the best-performing deep learning model: DNN. SHAP explanations can be mainly divided into Global and local SHAP explanations. The global explanation provides an overview of the model-in-whole and how each feature affects decision-making while local explanations explain a

Table 4
Performance indices neural networks.

Model	Phase	R^2	MAE	MSE	FB	MAPE
DNN	Training	0.977	1.93	6.00	−0.051	3.4
	Validation	0.982	1.33	3.11	−0.023	4.0
	Testing	0.972	1.93	5.93	−0.051	3.7
CNN	Training	0.939	2.51	9.26	−0.006	8.9
	Validation	0.928	2.83	11.63	0.002	8.7
	Testing	0.94	2.51	9.11	−0.019	8.6
ANN	Training	0.864	3.80	20.52	−0.008	12.1
	Validation	0.864	4.09	24.70	0.005	13.6
	Testing	0.854	3.92	22.27	−0.038	11.4

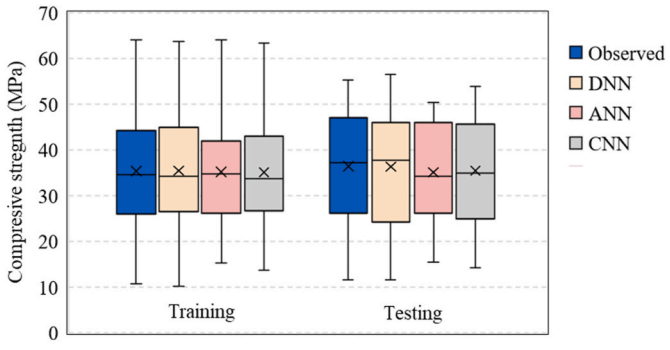

Fig. 6. Box plots for the training and testing predictions.

specific instance that users are interested in. Moreover, feature dependencies were obtained to understand the underlying contributions of each feature towards predictions.

5.1. Global explanations

Fig. 7 presents a detailed exposition of each variable's influence on the output, specifically the DNN model's estimation of compressive strength. Curing days were observed as the most impactful variable in predicting compressive strength. Fonseka & Nanayakkara [79] reported that a longer curing period has a strong impact on the early strength gain of concrete. Corncob ash is ranked second in SHAP global explanations and it negatively impacts compressive strength, whereas an increase in corncob ash decreases compressive strength. A similar conclusion has been drawn by Memon et al. in their experimental study [80]. The SHAP explanations revealed that higher ground-granulated blast furnace slag amounts increase the compressive strength of concrete. This finding can be validated by the experimental results of Hussain et al. who uncovers that the formation of C–S–H gel in ground-granulated blast furnace slag reaction increases the compressive strength [81]. Following ground-granulated blast furnace slag, fine aggregate content was chosen by SHAP as the next governing variable. However, the SHAP values of fine aggregate showcase a mixed variation, whereas higher fine aggregate content decreases the compressive strength. This agrees with what is generally observed in concrete behavior as described in section 3.4. An increase in fine aggregate results in a higher water-to-cement ratio that can make the cement paste weak. The remaining variables had a comparatively lower impact on the compressive strength of concrete. This is primarily due to the dataset's sample variance of feature values. Therefore, the explanation has to rely on a few values, as shown in Fig. 7.

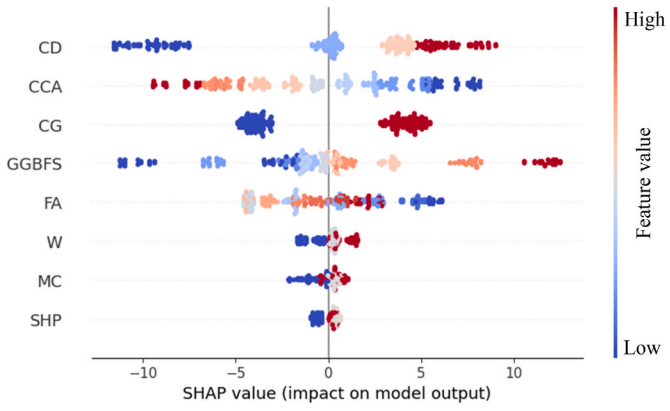

Fig. 7. SHAP global explanation obtained for DNN model (ground granulated blast furnace slag, GGBFS; corncob ash, CCA; fine aggregates, FA; water, W; sodium hydroxide pellets, SHP; curing days, CD; molarity concentrations, MC; concrete strength grade, CG).

Fig. 8 illustrates the average importance of features of the DNN model, with positive impacts (increase the compressive strength) indicated in red and negative impacts (decrease the compressive strength) indicated in blue. The feature curing days demonstrate a significant positive impact on compressive strength. Ground granulated blast furnace slag also has a notable impact, although its impact is lower than the impact of curing days. Fine aggregates, corncob ash, and molarity concentrations negatively impact compressive strength, implying an increase in feature would decrease compressive strength. Sodium hydroxide pellets have the lowest positive impact on the model predictions.

Following that, the explanations were divided based on the curing period as it was the most dominant feature in the dataset. Fig. 9 illustrates the mean absolute SHAP value obtained for each group. At curing days = 7 days, Ground granulated blast furnace slag showcases a positive impact on compressive strength. Ground granulated blast furnace slag is known for its pozzolanic properties which contribute to early strength gain through the formation of additional C–S–H gel [81]. The negative impact of fine aggregate could be due to the increased surface area of fine aggregates which requires more water, leading to a higher water-to-cement ratio and potentially a lower compressive strength. After 7 and 28 curing days, the effect of corncob ash becomes comparatively smaller.

With longer curing (after 56 days), the corncob ash content results in a decrease in compressive strength. This was reported by Memon et al. [80] as a result of the weaker mechanical properties of corncob ash. They have recommended replacing 10 % fine aggregates with corncob ash for the concrete mix. At 90 days of the curing period, the fine aggregate content has resulted in lower compressive strength and ground granulated blast furnace slag has shown a positive impact on the compressive strength. Shariq et al. [82] also reported that ground

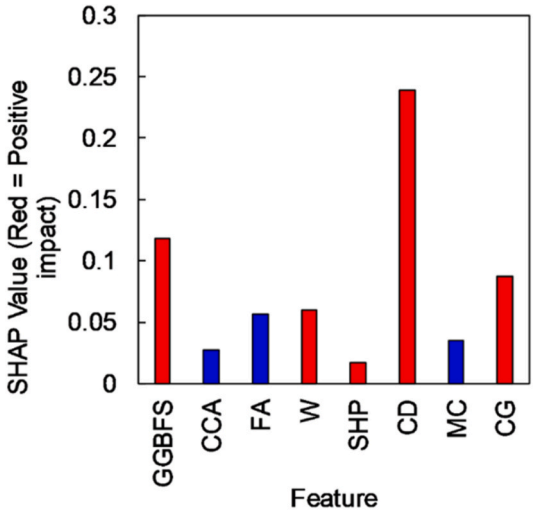

Fig. 8. Mean absolute SHAP values obtained for the DNN Model.

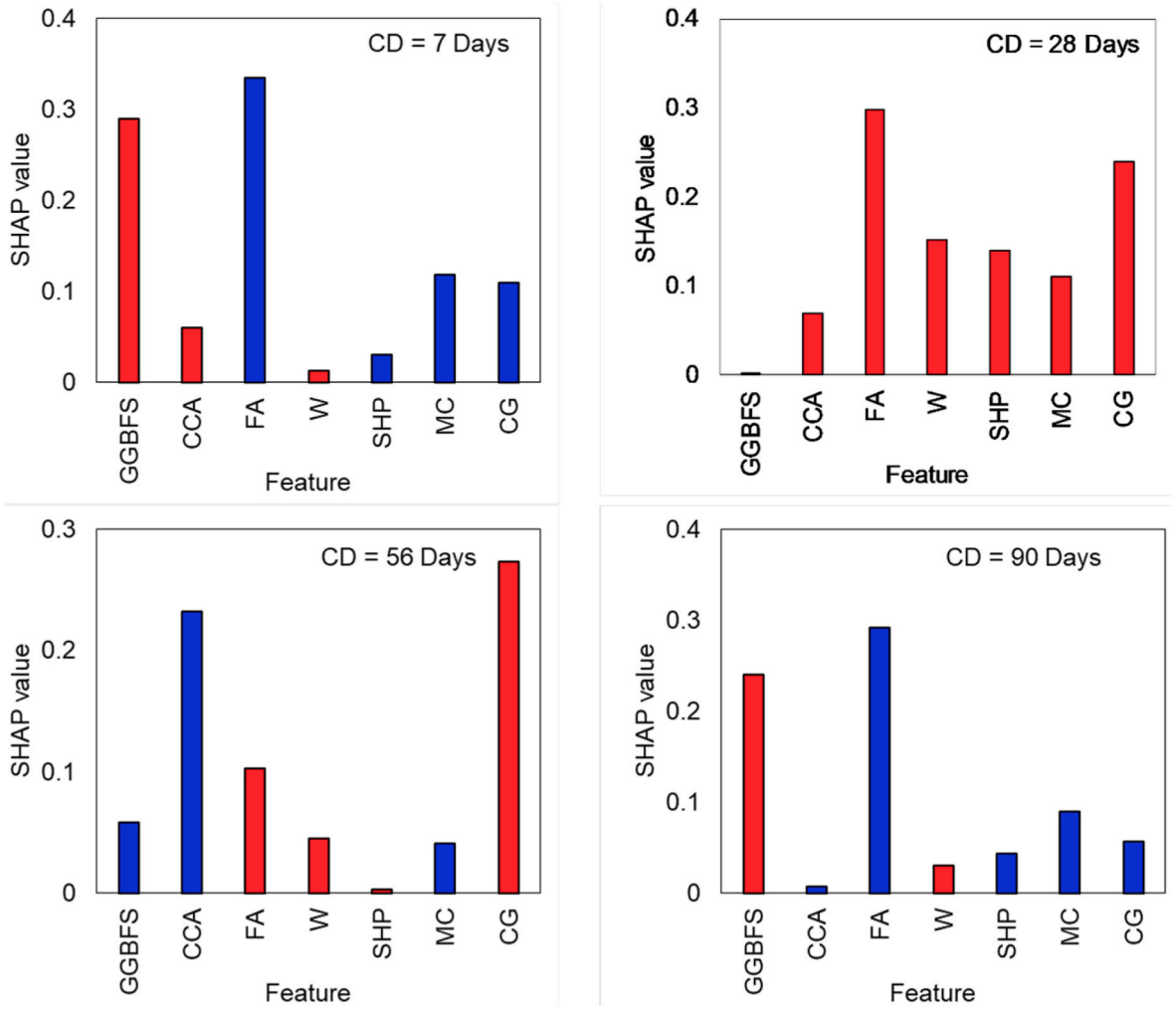

Fig. 9. Mean Absolute SHAP values obtained for explanation grouped based on curing period (Red: positive impact). (For interpretation of the references to colour in this figure legend, the reader is referred to the Web version of this article.)

granulated blast furnace slag is effective in strength gain at later stages compared to conventional concrete which agrees with the SHAP explanation.

A notable difference in the pair-wise correlations (Fig. 3) and SHAP explanations of the DNN model was observed in this study, in contrast to the similarity observed in classical machine learning studies [11,83,84]. For example, curing days indicated a low correlation with compressive strength whereas the SHAP explanation indicated curing days as the highest impactful parameter. One reason for this difference can be the normalization of feature magnitudes during the feature scaling process, in contrast to the actual values used in the pairwise correlation plot. In addition, the author's previous work uncovered that ***the SHAP explanations change for various classical machine-learning models despite their accuracy*** [12]. This conclusion may also apply to the difference identified in the feature importance between pair-wise correlation and SHAP explanation, thus the authors recommend to investigate variations in SHAP explanation for different classical machine learning and deep learning models in future works.

5.2. Local explanations

Although the SHAP global explanation provides a holistic view of how the DNN model predicts compressive strength with 8 parameters, real-world applications may need to study particular instances. The local explanation from SHAP is important in such scenarios. In this part of the study, the authors used six random points across the dataset and used the SHAP local explainer on those points as shown in Fig. 10. The parametric values of each instance (i.e. mix design values of 8 parameters) are shown in Table 5.

The results showcase the influence of various components on the compressive strength of concrete across six random instances. Instance 1 presents a compressive strength of 11.56 MPa with 7 days of curing. The absence of ground granulated blast furnace slag (0) and high Corncob Ash content indicated negative SHAP values on the prediction. Instance 2, which has a predicted strength of 32.9 MPa, notices an inclusion of ground granulated blast furnace slag content as per the positive SHAP values, increasing the compressive strength despite the lower curing period having a negative impact.

Instance 3, with a compressive strength of 45.2 MPa, displays the effect of increased curing days, moving the SHAP value for curing days into the positive, indicating a strong impact from extended curing time on the compressive strength. Instance 4, exhibiting a compressive strength of 55.2 MPa, shows a considerable positive impact from both ground granulated blast furnace slag and curing days as reflected in their SHAP values. In Instance 5, the highest compressive strength of 64 MPa is strongly dependent on ground granulated blast furnace slag and curing days, which align with the global model indicating positive SHAP values. Conversely, instance 6 demonstrates a drop in strength to 55.9 MPa. A similar variation of SHAP values is also observed compared to Instance 5. Overall, the local explanations present valuable insights into

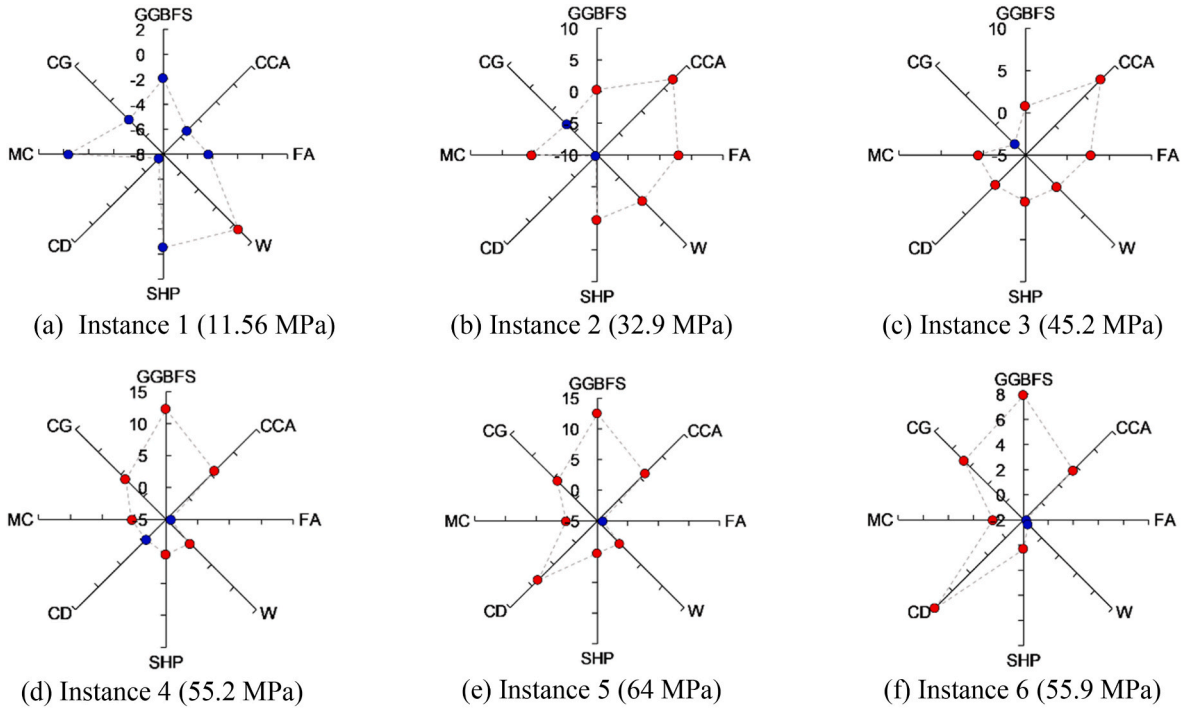

Fig. 10. Local explanations by SHAP on selected instances (predicted strength is mentioned within brackets).

Table 5
Selected instances for the location explanations.

Instance	GGBFS	CCA	FA	W	SHP	CD	MC	CG
1	0	380	841	37.86	20.74	7	12	30
2	380	0	899	35.16	23.44	7	14	30
3	380	0	899	35.16	23.44	28	14	30
4	488	0	805	35.16	23.44	28	14	40
5	390	98	788	32.64	25.96	90	16	40
6	488	0	805	35.16	23.44	90	14	40

a selected instance. Also, it is noteworthy that the local explanation need not always follow the global explanation.

5.3. Feature dependencies

Fig. 11 presents feature dependency plots for four selected features. A dependency plot is useful in identifying the impact of a variable in its full range. Here, it should be noteworthy that the DNNs were trained, validated, and tested using normalized input data. For a given feature, the minimum value of the feature is deducted and subsequently divided by the difference between the minimum and maximum of that feature. Scaling (normalization) ensures better performance in neural network models.

For this comparison, the x-axis (feature value) was re-converted into the original values for readers' convenience. Both curing days and ground granulated blast furnace slag showcase a positive impact (increases the compressive strength) over its full range. The SHAP values of each feature vary from −15 to 15, showing a significant impact on the compressive strength of geopolymer concrete. However, between 40 and 60 days in curing, the SHAP values are relatively lower, and a similar observation is obtained for values between 200 and 300 for ground granulated blast furnace slag. The remaining plots represent the effect of fine aggregates and corncob ash, respectively. An increase in corncob ash would result in a decrease in compressive strength. For fine aggregates, there is an optimum content where (800–850) the compressive strength would be minimized. Fine aggregate contents away from the optimum region showcased an increase in compressive strength. However, the lower fine aggregate content has resulted in the highest impact on compressive strength compared to the highest fine aggregate content.

Accordingly, the SHAP explanations were useful in identifying the trends in data and the decision-making process of the DNN. The explanations overall agreed with the physical reasoning obtained from related work. Using deep learning methods in structural engineering applications can assist in identifying complex patterns in data, helping practitioners in decision-making. The XAI method provides a required add-in to these black-box models by revealing their underlying reasoning. It improves the trust of domain experts and end users in these machine learning-based applications. The authors point out that not only the accuracy but also the explainability of the model should be achieved in order to implement these techniques in engineering applications.

6. Software interface to determine eco-friendly concrete mix design

The selection of the best deep learning model: DNN and the verification of its compressive strength prediction with the aid of SHAP demonstrate the importance and accuracy of using deep learning for concrete compressive strength predictions. This step followed a common forward workflow to develop an accurate deep-learning model in which various concrete mixes (different combinations of 8 parameters of geopolymer concrete ingredients) are used to predict compressive strength. However, the backward workflow which determines the concrete mix (suitable values of 8 parameters) for a given target compressive strength, is meaningful in practical civil engineering applications. This approach is also called inverse modeling in recent deep learning studies for engineering applications [85,86]. By following a similar approach, the authors developed an open-source software interface, that takes target compressive strength, and error margin as inputs, and provides concrete mix designs with the amount of each constituent (parameter) to achieve the design strength within the error margin. The interface is written in Python (Tkinter library [87]) and the source code is available in an online repository called CSpredictor [88]. The authors intend to add further developments to this tool in future research work.

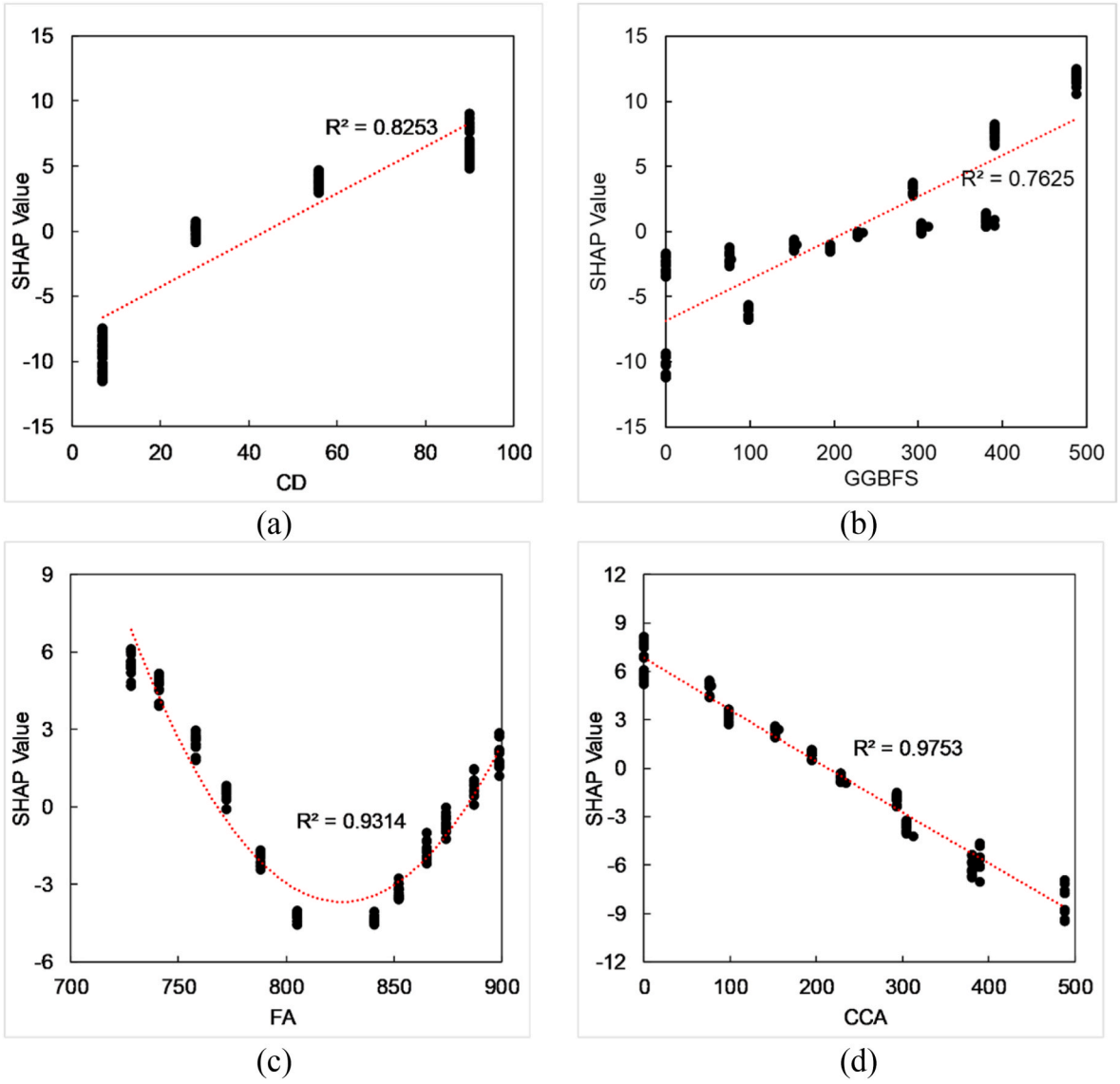

Fig. 11. Feature Dependency Plots (a) Curing days, (b) Ground granulated blast furnace slag, (c) Fine aggregates, and (d) Corncob ash.

The algorithm's execution sequence and a sample user interface are shown in Fig. 12.

The best deep learning model: DNN was chosen as the main predicting model in this software tool. First, the DNN model was trained using the whole (100 %) dataset, since its accuracy was well-proven in the analysis of this research. Then, the input dataset was divided into a large number of synthetic points. Let a, and b are the minimum and maximum of a given feature. If a specific input variable has 10 different values between a and b, that variable can be divided into 1000 or any larger number between a and b. Likewise, each feature is divided into a large number within its corresponding maximum and minimum values. The reason for this division is to cover the multidimensional sample space as the DNN model has accurately captured its relationship with the Compressive Strength. The algorithm first generates 1000 (the number used for the division) random concrete mixes (combinations of 8 parameters). Subsequently, the compressive strength is predicted for each mix by calling the DNN model.

Then algorithm evaluates whether there are at least five feasible solutions, in other words, concrete mixes that archive target compressive strength within the given error margin. Finally, an additional parameter: Global Warming Potential (GWP) is calculated for each feasible concrete mix and sorted in ascending order whereas the concrete mix with the lowest GWP is proposed as the first choice. GWP is a frequently cited parameter for sustainable concrete mixes that is aimed at minimising global warming in concrete production process [89,90]. GWP calculation of this study was constrained by the cradle-to-gate system boundary and the GWP (in terms of $kgCO_2$ equivalent) of each material was obtained from a recent study conducted by Oyebisi et al. [91]. To demonstrate a practical use case of this interface, the most sustainable concrete mix for 35 MPa target strength is shown in Table 6. The software tool developed in this study demonstrates two important aspects. First, this is a ready-to-use tool for engineers who are interested in investigating slag-ash-based geopolymer concrete mixes for a target compressive strength. Second, the inverse modeling approach is useful for future research aimed at developing practical applications based on deep learning algorithms.

7. Conclusion

The study developed three deep learning algorithms to predict the compressive strength of slag-ash-based geopolymer concrete. The model performances revealed that the Deep Neural Network(DNN) algorithm is the best-performing model. Subsequently, Shapley additive explanations were employed to interpret model predictions of Deep Neural

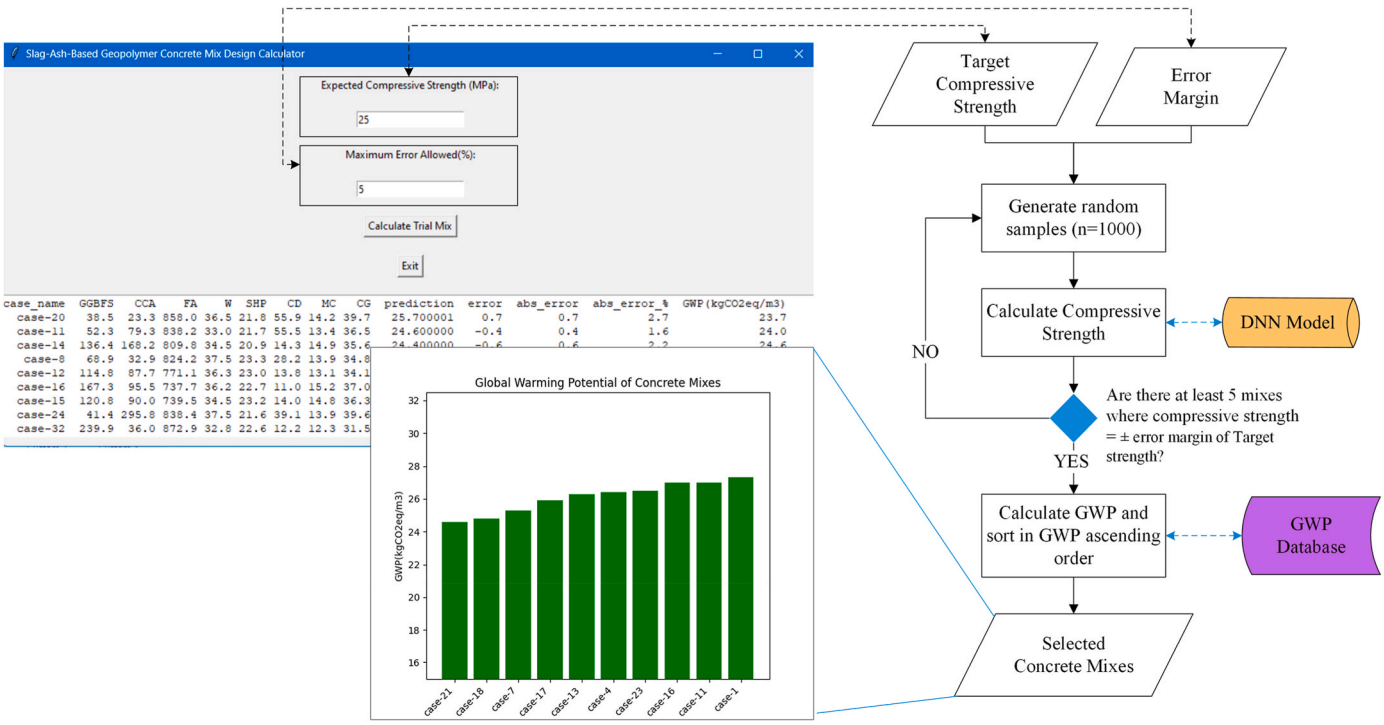

Fig. 12. The novel software tool to obtain a mixed design of slag ash-based geopolymer concrete with its global warming potential.

Table 6
Proposed concrete mixes for target compressive strengths of 35 MPa.

Target compressive strength (MPa)	Concrete mix (kg/m^3)	Global Warming Potential (kg CO_2eq/ m^3)
35	• Ground Granulated Blast Furnace Slag-129.2 •Corncob Ash - 93.5 •Fine Aggregates – 806.6 •Water - 33.7 •Sodium Hydroxide Pellets – 20.8 •Molarity Concentrations – 15.2 •*Curing days: 28*	23.8

Networks (DNN). Moreover, the authors developed a software interface that can predict the eco-friendly, slag-ash-based geopolymer concrete mix that achieves a given target compressive strength. The findings of the study demonstrate the importance of explaining model interpretations of deep learning models and the viability of preparing practical software tools.

- Deep learning algorithms effectively capture the non-linear behavior of strength characteristics in slag-ash-based geopolymer concrete. Out of three deep learning models, the Deep Neural Network (DNN) model achieved a high accuracy, with R^2 values of 0.977 for training and 0.972 for testing. However, the accuracy of the other two models, Convolutional Neural Network (CNN) and Artificial Neural Network (ANN), was lower, with R^2 values of 0.939 for training and 0.94 for testing for the CNN, and 0.864 for training and 0.869 for testing for the ANN.
- Shapley Additive Explanations (SHAP) analysis on the Deep Neural Network (DNN) model revealed that curing days, followed by Ground Granulated Blast Furnace Slag, are the most dominant features when predicting compressive strength. It also found that Sodium Hydroxide Pellets contribute weakly to compressive strength. The comparison of SHAP results with recent experimental-based studies confirms the accuracy of these interpretations.
- The inverse modeling technique has proven useful in employing deep learning models for practical engineering applications. Although this study demonstrated its application using a straightforward approach, the viability, accuracy, and efficiency of this technique should be further studied in future work, particularly in the context of concrete strength predictions.

CRediT authorship contribution statement

R.S.S. Ranasinghe: Writing – original draft, Validation, Methodology, Data curation. **W.K.V.J.B. Kulasooriya:** Writing – original draft, Validation, Methodology. **Udara Sachinthana Perera:** Writing – review & editing, Validation, Methodology. **I.U. Ekanayake:** Writing – review & editing, Validation, Resources, Conceptualization. **D.P.P. Meddage:** Writing – review & editing, Validation, Conceptualization. **Damith Mohotti:** Writing – review & editing, Supervision, Conceptualization. **Upaka Rathanayake:** Writing – review & editing, Supervision, Funding acquisition.

Declaration of competing interest

The authors declare that they have no known competing financial interests or personal relationships that could have appeared to influence the work reported in this paper.

Data availability

Data will be made available on request.

References

[1] IEA, Direct emissions intensity of cement production in the Net Zero Scenario, 2015-2030 – Charts – Data & Statistics, IEA. Accessed: Jan. 22, 2024. [Online]. Available: https://www.iea.org/data-and-statistics/charts/direct-emissions-intensity-of-cement-production-in-the-net-zero-scenario-2015-2030-2.

[2] A.L. Almutairi, B.A. Tayeh, A. Adesina, H.F. Isleem, A.M. Zeyad, Potential applications of geopolymer concrete in construction: a review, Dec, Case Stud. Constr. Mater. 15 (2021) e00733, https://doi.org/10.1016/j.cscm.2021.e00733.
[3] B. Singh, G. Ishwarya, M. Gupta, S.K. Bhattacharyya, Geopolymer concrete: a review of some recent developments, Jun, Construct. Build. Mater. 85 (2015) 78–90, https://doi.org/10.1016/j.conbuildmat.2015.03.036.
[4] P. Duxson, A. Fernández-Jiménez, J.L. Provis, G.C. Lukey, A. Palomo, J.S.J. van Deventer, Geopolymer technology: the current state of the art, May, J. Mater. Sci. 42 (9) (2007) 2917–2933, https://doi.org/10.1007/s10853-006-0637-z.
[5] P. Muthuramalingam, B. Dharmar, P.V.S. Babu, Investigation on the study of durability characteristics and endurance of phosphate-admixed geopolymer concrete incorporated with copper slag, Apr, Iran J Sci Technol Trans Civ Eng 47 (2) (2023) 819–828, https://doi.org/10.1007/s40996-022-00921-x.
[6] E.I. Diaz-Loya, Mechanical properties of fly-ash-based geopolymer concrete - ProQuest. https://www.proquest.com/openview/f5f71d0d193e113ad4295caa60b3f346/1?pq-origsite=gscholar&cbl=37076. (Accessed 17 September 2023).
[7] M. Olivia, H. Nikraz, Properties of fly ash geopolymer concrete designed by Taguchi method, Apr, Mater. Des. 36 (2012) 191–198, https://doi.org/10.1016/j.matdes.2011.10.036.
[8] M. Rahmati, V. Toufigh, Evaluation of geopolymer concrete at high temperatures: an experimental study using machine learning, Oct, J. Clean. Prod. 372 (2022) 133608, https://doi.org/10.1016/j.jclepro.2022.133608.
[9] K.T. Nguyen, Q.D. Nguyen, T.A. Le, J. Shin, K. Lee, Analyzing the compressive strength of green fly ash based geopolymer concrete using experiment and machine learning approaches, Jun, Construct. Build. Mater. 247 (2020) 118581, https://doi.org/10.1016/j.conbuildmat.2020.118581.
[10] Y. Peng, C. Unluer, Analyzing the mechanical performance of fly ash-based geopolymer concrete with different machine learning techniques, Jan, Construct. Build. Mater. 316 (2022) 125785, https://doi.org/10.1016/j.conbuildmat.2021.125785.
[11] I.U. Ekanayake, D.P.P. Meddage, U. Rathnayake, A novel approach to explain the black-box nature of machine learning in compressive strength predictions of concrete using Shapley additive explanations (SHAP), Jun, Case Stud. Constr. Mater. 16 (2022) e01059, https://doi.org/10.1016/j.cscm.2022.e01059.
[12] W.K.V.J.B. Kulasooriya, R.S.S. Ranasinghe, U.S. Perera, P. Thisovithan, I. U. Ekanayake, D.P.P. Meddage, Modeling strength characteristics of basalt fiber reinforced concrete using multiple explainable machine learning with a graphical user interface, Aug, Sci. Rep. 13 (1) (2023) 13138, https://doi.org/10.1038/s41598-023-40513-x.
[13] G. Pazouki, Fly ash-based geopolymer concrete's compressive strength estimation by applying artificial intelligence methods, Nov, Measurement 203 (2022) 111916, https://doi.org/10.1016/j.measurement.2022.111916.
[14] K.T. Nguyen, Q.D. Nguyen, T.A. Le, J. Shin, K. Lee, Analyzing the compressive strength of green fly ash based geopolymer concrete using experiment and machine learning approaches, Jun, Construct. Build. Mater. 247 (2020) 118581, https://doi.org/10.1016/j.conbuildmat.2020.118581.
[15] Y. Peng, C. Unluer, Analyzing the mechanical performance of fly ash-based geopolymer concrete with different machine learning techniques, Jan, Construct. Build. Mater. 316 (2022) 125785, https://doi.org/10.1016/j.conbuildmat.2021.125785.
[16] A.A. Shahmansouri, M. Yazdani, S. Ghanbari, H. Akbarzadeh Bengar, A. Jafari, H. Farrokh Ghatte, Artificial neural network model to predict the compressive strength of eco-friendly geopolymer concrete incorporating silica fume and natural zeolite, Jan, J. Clean. Prod. 279 (2021) 123697, https://doi.org/10.1016/j.jclepro.2020.123697.
[17] W. Huo, Z. Zhu, H. Sun, B. Ma, L. Yang, Development of machine learning models for the prediction of the compressive strength of calcium-based geopolymers, Dec, J. Clean. Prod. 380 (2022) 135159, https://doi.org/10.1016/j.jclepro.2022.135159.
[18] M. Rahmati, V. Toufigh, Evaluation of geopolymer concrete at high temperatures: an experimental study using machine learning, Oct, J. Clean. Prod. 372 (2022) 133608, https://doi.org/10.1016/j.jclepro.2022.133608.
[19] A. Ahmad, W. Ahmad, F. Aslam, P. Joyklad, Compressive strength prediction of fly ash-based geopolymer concrete via advanced machine learning techniques, Jun, Case Stud. Constr. Mater. 16 (2022) e00840, https://doi.org/10.1016/j.cscm.2021.e00840.
[20] A.T. Huynh, et al., A machine learning-assisted numerical predictor for compressive strength of geopolymer concrete based on experimental data and sensitivity analysis, Jan, Appl. Sci. 10 (21) (2020), https://doi.org/10.3390/app10217726.
[21] R. Cao, Z. Fang, M. Jin, Y. Shang, Application of machine learning approaches to predict the strength property of geopolymer concrete, Jan, Materials 15 (7) (2022), https://doi.org/10.3390/ma15072400.
[22] C. Cakiroglu, K. Islam, G. Bekdaş, U. Isikdag, S. Mangalathu, Explainable machine learning models for predicting the axial compression capacity of concrete filled steel tubular columns, Nov, Construct. Build. Mater. 356 (2022) 129227, https://doi.org/10.1016/j.conbuildmat.2022.129227.
[23] D. Chakraborty, I. Awolusi, L. Gutierrez, An explainable machine learning model to predict and elucidate the compressive behavior of high-performance concrete, Sep, Results in Engineering 11 (2021) 100245, https://doi.org/10.1016/j.rineng.2021.100245.
[24] J.-H. Choi, D. Kim, M.-S. Ko, D.-E. Lee, K. Wi, H.-S. Lee, Compressive strength prediction of ternary-blended concrete using deep neural network with tuned hyperparameters, Sep, J. Build. Eng. 75 (2023) 107004, https://doi.org/10.1016/j.jobe.2023.107004.
[25] S. Oyebisi, T. Alomayri, Artificial intelligence-based prediction of strengths of slag-ash-based geopolymer concrete using deep neural networks, Oct, Construct. Build. Mater. 400 (2023) 132606, https://doi.org/10.1016/j.conbuildmat.2023.132606.
[26] M.M. Moein, A. Soliman, Predicting the compressive strength of alkali-activated concrete using various data mining methods, in: S. Walbridge, M. Nik-Bakht, K.T. W. Ng, M. Shome, M.S. Alam, A. el Damatty, G. Lovegrove (Eds.), Proceedings of the Canadian Society of Civil Engineering Annual Conference 2021, Lecture Notes in Civil Engineering, Singapore: Springer Nature, 2023, pp. 317–326, https://doi.org/10.1007/978-981-19-1004-3_26.
[27] H.U. Ahmed, A.S. Mohammed, S.M.A. Qaidi, R.H. Faraj, N. Hamah Sor, A. A. Mohammed, Compressive strength of geopolymer concrete composites: a systematic comprehensive review, analysis and modeling, Feb, European Journal of Environmental and Civil Engineering 27 (3) (2023) 1383–1428, https://doi.org/10.1080/19648189.2022.2083022.
[28] H.U. Ahmed, et al., Innovative modeling techniques including MEP, ANN and FQ to forecast the compressive strength of geopolymer concrete modified with nanoparticles, Jun, Neural Comput. Appl. 35 (17) (2023) 12453–12479, https://doi.org/10.1007/s00521-023-08378-3.
[29] H. Unis Ahmed, A.S. Mohammed, A.A. Mohammed, Fresh and mechanical performances of recycled plastic aggregate geopolymer concrete modified with Nano-silica: experimental and computational investigation, Aug, Construct. Build. Mater. 394 (2023) 132266, https://doi.org/10.1016/j.conbuildmat.2023.132266.
[30] H.U. Ahmed, A.A. Mohammed, A. Mohammed, Soft computing models to predict the compressive strength of GGBS/FA- geopolymer concrete, May, PLoS One 17 (2022) e0265846, https://doi.org/10.1371/journal.pone.0265846.
[31] V.W.Y. Tam, A. Butera, K.N. Le, L.C.F.D. Silva, A.C.J. Evangelista, A prediction model for compressive strength of CO2 concrete using regression analysis and artificial neural networks, Mar, Construct. Build. Mater. 324 (2022) 126689, https://doi.org/10.1016/j.conbuildmat.2022.126689.
[32] H.-B. Ly, T.-A. Nguyen, H.-V. Thi Mai, V.Q. Tran, Development of deep neural network model to predict the compressive strength of rubber concrete, Sep, Construct. Build. Mater. 301 (2021) 124081, https://doi.org/10.1016/j.conbuildmat.2021.124081.
[33] F. Farooq, W. Ahmed, A. Akbar, F. Aslam, R. Alyousef, Predictive modeling for sustainable high-performance concrete from industrial wastes: a comparison and optimization of models using ensemble learners, Apr, J. Clean. Prod. 292 (2021) 126032, https://doi.org/10.1016/j.jclepro.2021.126032.
[34] A. Mahmoodzadeh, et al., Artificial intelligence forecasting models of uniaxial compressive strength, Mar, Transportation Geotechnics 27 (2021) 100499, https://doi.org/10.1016/j.trgeo.2020.100499.
[35] E.M. Golafshani, A. Behnood, M. Arashpour, Predicting the compressive strength of normal and high-performance concretes using ANN and ANFIS hybridized with grey wolf optimizer, Jan, Construct. Build. Mater. 232 (2020) 117266, https://doi.org/10.1016/j.conbuildmat.2019.117266.
[36] A.T. Huynh, et al., A machine learning-assisted numerical predictor for compressive strength of geopolymer concrete based on experimental data and sensitivity analysis, Oct, Appl. Sci. 10 (21) (2020) 7726, https://doi.org/10.3390/app10217726.
[37] D.V. Dao, H.-B. Ly, S.H. Trinh, T.-T. Le, B.T. Pham, Artificial intelligence approaches for prediction of compressive strength of geopolymer concrete, Jan, Materials 12 (6) (2019), https://doi.org/10.3390/ma12060983.
[38] P.G. Asteris, K.G. Kolovos, Self-compacting concrete strength prediction using surrogate models, Jan, Neural Comput. Appl. 31 (1) (2019) 409–424, https://doi.org/10.1007/s00521-017-3007-7.
[39] M.A. Getahun, S.M. Shitote, Z.C. Abiero Gariy, Artificial neural network based modelling approach for strength prediction of concrete incorporating agricultural and construction wastes, Nov, Construct. Build. Mater. 190 (2018) 517–525, https://doi.org/10.1016/j.conbuildmat.2018.09.097.
[40] H. Naderpour, A.H. Rafiean, P. Fakharian, Compressive strength prediction of environmentally friendly concrete using artificial neural networks, Mar, J. Build. Eng. 16 (2018) 213–219, https://doi.org/10.1016/j.jobe.2018.01.007.
[41] D.-K. Bui, T. Nguyen, J.-S. Chou, H. Nguyen-Xuan, T.D. Ngo, A modified firefly algorithm-artificial neural network expert system for predicting compressive and tensile strength of high-performance concrete, Aug, Construct. Build. Mater. 180 (2018) 320–333, https://doi.org/10.1016/j.conbuildmat.2018.05.201.
[42] S. Chithra, S.R.R.S. Kumar, K. Chinnaraju, F. Alfin Ashmita, A comparative study on the compressive strength prediction models for High Performance Concrete containing nano silica and copper slag using regression analysis and Artificial Neural Networks, Jul, Construct. Build. Mater. 114 (2016) 528–535, https://doi.org/10.1016/j.conbuildmat.2016.03.214.
[43] B.A. Omran, Q. Chen, R. Jin, Comparison of data mining techniques for predicting compressive strength of environmentally friendly concrete, Nov, J. Comput. Civ. Eng. 30 (6) (2016) 04016029, https://doi.org/10.1061/(ASCE)CP.1943-5487.0000596.
[44] P. Chopra, R.K. Sharma, M. Kumar, Prediction of compressive strength of concrete using artificial neural network and genetic programming, Adv. Mater. Sci. Eng. 2016 (2016) 1–10, https://doi.org/10.1155/2016/7648467.
[45] N. Deshpande, S. Londhe, S. Kulkarni, Modeling compressive strength of recycled aggregate concrete by artificial neural network, model tree and non-linear regression, Dec, International Journal of Sustainable Built Environment 3 (2) (2014) 187–198, https://doi.org/10.1016/j.ijsbe.2014.12.002.
[46] Z.H. Duan, S.C. Kou, C.S. Poon, Prediction of compressive strength of recycled aggregate concrete using artificial neural networks, Mar, Construct. Build. Mater. 40 (2013) 1200–1206, https://doi.org/10.1016/j.conbuildmat.2012.04.063.
[47] A.T.A. Dantas, M. Batista Leite, K. De Jesus Nagahama, Prediction of compressive strength of concrete containing construction and demolition waste using artificial

neural networks, Jan, Construct. Build. Mater. 38 (2013) 717–722, https://doi.org/10.1016/j.conbuildmat.2012.09.026.
[48] M. Uysal, H. Tanyildizi, Estimation of compressive strength of self compacting concrete containing polypropylene fiber and mineral additives exposed to high temperature using artificial neural network, Feb, Construct. Build. Mater. 27 (1) (2012) 404–414, https://doi.org/10.1016/j.conbuildmat.2011.07.028.
[49] R. Siddique, P. Aggarwal, Y. Aggarwal, Prediction of compressive strength of self-compacting concrete containing bottom ash using artificial neural networks, Oct, Adv. Eng. Software 42 (10) (2011) 780–786, https://doi.org/10.1016/j.advengsoft.2011.05.016.
[50] C. Deepa, K. SathiyaKumari, V.P. Sudha, Prediction of the compressive strength of high performance concrete mix using tree based modeling, Sep, IJCA 6 (5) (2010) 18–24, https://doi.org/10.5120/1076-1406.
[51] C. Bilim, C.D. Atiş, H. Tanyildizi, O. Karahan, Predicting the compressive strength of ground granulated blast furnace slag concrete using artificial neural network, May, Adv. Eng. Software 40 (5) (2009) 334–340, https://doi.org/10.1016/j.advengsoft.2008.05.005.
[52] M.M. Alshihri, A.M. Azmy, M.S. El-Bisy, Neural networks for predicting compressive strength of structural light weight concrete, Jun, Construct. Build. Mater. 23 (6) (2009) 2214–2219, https://doi.org/10.1016/j.conbuildmat.2008.12.003.
[53] M. Sarıdemir, İ.B. Topçu, F. Özcan, M.H. Severcan, Prediction of long-term effects of GGBFS on compressive strength of concrete by artificial neural networks and fuzzy logic, Mar, Construct. Build. Mater. 23 (3) (2009) 1279–1286, https://doi.org/10.1016/j.conbuildmat.2008.07.021.
[54] İ.B. Topçu, M. Sarıdemir, Prediction of compressive strength of concrete containing fly ash using artificial neural networks and fuzzy logic, Jan, Comput. Mater. Sci. 41 (3) (2008) 305–311, https://doi.org/10.1016/j.commatsci.2007.04.009.
[55] M.H. Fazel Zarandi, I.B. Türksen, J. Sobhani, A.A. Ramezanianpour, Fuzzy polynomial neural networks for approximation of the compressive strength of concrete, Jan, Appl. Soft Comput. 8 (1) (2008) 488–498, https://doi.org/10.1016/j.asoc.2007.02.010.
[56] F. Altun, Ö. Kişi, K. Aydin, Predicting the compressive strength of steel fiber added lightweight concrete using neural network, Apr, Comput. Mater. Sci. 42 (2) (2008) 259–265, https://doi.org/10.1016/j.commatsci.2007.07.011.
[57] M. Pala, E. Özbay, A. Öztaş, M.I. Yuce, Appraisal of long-term effects of fly ash and silica fume on compressive strength of concrete by neural networks, Feb, Construct. Build. Mater. 21 (2) (2007) 384–394, https://doi.org/10.1016/j.conbuildmat.2005.08.009.
[58] A. Öztaş, M. Pala, E. Özbay, E. Kanca, N. Çaglar, M.A. Bhatti, Predicting the compressive strength and slump of high strength concrete using neural network, Nov, Construct. Build. Mater. 20 (9) (2006) 769–775, https://doi.org/10.1016/j.conbuildmat.2005.01.054.
[59] W.P.S. Dias, S.P. Pooliyadda, Neural networks for predicting properties of concretes with admixtures, Oct, Construct. Build. Mater. 15 (7) (2001) 371–379, https://doi.org/10.1016/S0950-0618(01)00006-X.
[60] H.-G. Ni, J.-Z. Wang, Prediction of compressive strength of concrete by neural networks, Aug, Cement Concr. Res. 30 (8) (2000) 1245–1250, https://doi.org/10.1016/S0008-8846(00)00345-8.
[61] A. Temenos, N. Temenos, M. Kaselimi, A. Doulamis, N. Doulamis, Interpretable deep learning framework for land use and land cover classification in remote sensing using SHAP, Geosci. Rem. Sens. Lett. IEEE 20 (2023) 1–5, https://doi.org/10.1109/LGRS.2023.3251652.
[62] A.T. Keleko, B. Kamsu-Foguem, R.H. Ngouna, A. Tongne, Health condition monitoring of a complex hydraulic system using Deep Neural Network and DeepSHAP explainable XAI, Jan, Adv. Eng. Software 175 (2023) 103339, https://doi.org/10.1016/j.advengsoft.2022.103339.
[63] S. Oyebisi, T. Alomayri, Artificial intelligence-based prediction of strengths of slag-ash-based geopolymer concrete using deep neural networks, Oct, Construct. Build. Mater. 400 (2023) 132606, https://doi.org/10.1016/j.conbuildmat.2023.132606.
[64] A. Géron, Hands-On Machine Learning with Scikit-Learn, Keras, and TensorFlow, O'Reilly Media, Inc., 2022.
[65] J.P.S.S. Madushani, R.M.K. Sandamal, D.P.P. Meddage, H.R. Pasindu, P.I. A. Gomes, Evaluating expressway traffic crash severity by using logistic regression and explainable & supervised machine learning classifiers, Sep, Transport Eng. 13 (2023) 100190, https://doi.org/10.1016/j.treng.2023.100190.
[66] C. Madhushani, K. Dananjaya, I.U. Ekanayake, D.P.P. Meddage, K. Kantamaneni, U. Rathnayake, Modeling streamflow in non-gauged watersheds with sparse data considering physiographic, dynamic climate, and anthropogenic factors using explainable soft computing techniques, Mar, J. Hydrol. 631 (2024) 130846, https://doi.org/10.1016/j.jhydrol.2024.130846.
[67] G. Dharmarathne, T.N. Jayasinghe, M. Bogahawaththa, D.P.P. Meddage, U. Rathnayake, A novel machine learning approach for diagnosing diabetes with a self-explainable interface, Jun, Healthcare Analytics 5 (2024) 100301, https://doi.org/10.1016/j.health.2024.100301.
[68] U.A.K.K. Perera, D.T.S. Coralage, I.U. Ekanayake, J. Alawatugoda, D.P.P. Meddage, A new frontier in streamflow modeling in ungauged basins with sparse data: a modified generative adversarial network with explainable AI, Mar, Results in Engineering 21 (2024) 101920, https://doi.org/10.1016/j.rineng.2024.101920.
[69] D.P.P. Meddage, I.U. Ekanayake, A.U. Weerasuriya, C.S. Lewangamage, Tree-based regression models for predicting external wind pressure of a building with an unconventional configuration, Jul, in: *2021 Moratuwa Engineering Research Conference (MERCon)*, Moratuwa, IEEE, Sri Lanka, 2021, pp. 257–262, https://doi.org/10.1109/MERCon52712.2021.9525734.
[70] D.P.P. Meddage, et al., Explainable Machine Learning (XML) to predict external wind pressure of a low-rise building in urban-like settings, Jul, J. Wind Eng. Ind. Aerod. 226 (2022) 105027, https://doi.org/10.1016/j.jweia.2022.105027.
[71] P. Meddage, I. Ekanayake, U.S. Perera, H.M. Azamathulla, M.A. Md Said, U. Rathnayake, Interpretation of machine-learning-based (Black-box) wind pressure predictions for low-rise gable-roofed buildings using Shapley additive explanations (SHAP), Jun, Buildings 12 (6) (2022), https://doi.org/10.3390/buildings12060734.
[72] D.P.P. Meddage, I.U. Ekanayake, S. Herath, R. Gobirahavan, N. Muttil, U. Rathnayake, Predicting bulk average velocity with rigid vegetation in open channels using tree-based machine learning: a novel approach using explainable artificial intelligence, Jan, Sensors 22 (12) (2022), https://doi.org/10.3390/s22124398.
[73] S.M. Lundberg, S.-I. Lee, A unified approach to interpreting model predictions, in: Advances in Neural Information Processing Systems, Curran Associates, Inc., 2017. Accessed: Jan. 24, 2024. [Online]. Available: https://proceedings.neurips.cc/paper/2017/hash/8a20a8621978632d76c43dfd28b67767-Abstract.html.
[74] D.P.P. Meddage, D. Mohotti, K. Wijesooriya, Predicting transient wind loads on tall buildings in three-dimensional spatial coordinates using machine learning, May, J. Build. Eng. 85 (2024) 108725, https://doi.org/10.1016/j.jobe.2024.108725.
[75] M.C. Chi, J.H. Chi, C.H. Wu, Effect of GGBFS on compressive strength and durability of concrete, Mar, AMR (Adv. Magn. Reson.) 1145 (2018) 22–26, https://doi.org/10.4028/www.scientific.net/AMR.1145.22.
[76] P. Nath, P.K. Sarker, Effect of GGBFS on setting, workability and early strength properties of fly ash geopolymer concrete cured in ambient condition, Sep, Construct. Build. Mater. 66 (2014) 163–171, https://doi.org/10.1016/j.conbuildmat.2014.05.080.
[77] S. Assefa, Production of lightweight concrete using corncob ash as replacement of cement in concrete, AJCE 7 (1) (2019) 17, https://doi.org/10.11648/j.ajce.20190701.13.
[78] R. Gustriansyah, D.I. Sensuse, A. Ramadhan, A sales prediction model adopted the recency-frequency-monetary concept, Jun, Indonesian Journal of Electrical Engineering and Computer Science 6 (3) (2017), https://doi.org/10.11591/ijeecs.v6.i3.pp711-720.
[79] N.H.I.C. Fonseka, S.M.A. Nanayakkara, Assessment of concrete durability by surface resistivity and initial surface absorption, in: R. Dissanayake, P. Mendis, K. Weerasekera, S. De Silva, S. Fernando, C. Konthesingha (Eds.), 12th International Conference on Structural Engineering and Construction Management, Springer Nature, Lecture Notes in Civil Engineering. Singapore, 2023, pp. 603–620, https://doi.org/10.1007/978-981-19-2886-4_43.
[80] S.A. Memon, U. Javed, R.A. Khushnood, Eco-friendly utilization of corncob ash as partial replacement of sand in concrete, Jan, Construct. Build. Mater. 195 (2019) 165–177, https://doi.org/10.1016/j.conbuildmat.2018.11.063.
[81] F. Hussain, I. Kaur, A. Hussain, Reviewing the influence of GGBFS on concrete properties, Mater. Today: Proc. 32 (Jan. 2020) 997–1004, https://doi.org/10.1016/j.matpr.2020.07.410.
[82] M. Shariq, J. Prasad, A. Masood, Effect of GGBFS on time dependent compressive strength of concrete, Aug, Construct. Build. Mater. 24 (8) (2010) 1469–1478, https://doi.org/10.1016/j.conbuildmat.2010.01.007.
[83] P. Thisovithan, H. Aththanayake, D.P.P. Meddage, I.U. Ekanayake, U. Rathnayake, A novel explainable AI-based approach to estimate the natural period of vibration of masonry infill reinforced concrete frame structures using different machine learning techniques, Sep, Results in Engineering 19 (2023) 101388, https://doi.org/10.1016/j.rineng.2023.101388.
[84] I.U. Ekanayake, S. Palitha, S. Gamage, D.P.P. Meddage, K. Wijesooriya, D. Mohotti, Predicting adhesion strength of micropatterned surfaces using gradient boosting models and explainable artificial intelligence visualizations, Aug, Mater. Today Commun. 36 (2023) 106545, https://doi.org/10.1016/j.mtcomm.2023.106545.
[85] C. Wanigasekara, E. Oromiehie, A. Swain, B.G. Prusty, S.K. Nguang, Machine learning-based inverse predictive model for AFP based thermoplastic composites, Jun, Journal of Industrial Information Integration 22 (2021) 100197, https://doi.org/10.1016/j.jii.2020.100197.
[86] M. Sedaghat, R. Trinchero, Z.H. Firouzeh, F.G. Canavero, Compressed machine learning-based inverse model for design optimization of microwave components, Jul, IEEE Trans. Microw. Theor. Tech. 70 (7) (2022) 3415–3427, https://doi.org/10.1109/TMTT.2022.3166151.
[87] tkinter — Python interface to Tcl/Tk," Python documentation. Accessed: May 25, 2024. [Online]. Available: https://docs.python.org/3/library/tkinter.html.
[88] U.S. Perera, D.P.P. Meddage, I.U. Ekanayake, R.S.S. Ranasinghe, W.K.J. B. Kulasooriya, CSpredictor. https://github.com/Udaragithub/CSpredictor, 2024.
[89] S.A. Miller, P.J.M. Monteiro, C.P. Ostertag, A. Horvath, Concrete mixture proportioning for desired strength and reduced global warming potential, Dec, Construct. Build. Mater. 128 (2016) 410–421, https://doi.org/10.1016/j.conbuildmat.2016.10.081.
[90] R. Kurad, J.D. Silvestre, J. de Brito, H. Ahmed, Effect of incorporation of high volume of recycled concrete aggregates and fly ash on the strength and global warming potential of concrete, Nov, J. Clean. Prod. 166 (2017) 485–502, https://doi.org/10.1016/j.jclepro.2017.07.236.
[91] S. Oyebisi, et al., Sustainability assessment of geopolymer concrete synthesized by slag and corncob ash, Dec, Case Stud. Constr. Mater. 17 (2022) e01665, https://doi.org/10.1016/j.cscm.2022.e01665.